

THE RELATIONSHIP OF TOPOGRAPHIC WAVES
ON THE CONTINENTAL RISE
TO GULF STREAM FLUCTUATIONS

by

Elizabeth Burch Welsh

B.A., College of William and Mary, Williamsburg, VA
(1980)

SUBMITTED TO THE DEPARTMENT OF EARTH,
ATMOSPHERIC AND PLANETARY SCIENCES
IN PARTIAL FULFILLMENT
OF THE REQUIREMENTS FOR THE
DEGREE OF

MASTER OF SCIENCE IN
PHYSICAL OCEANOGRAPHY

at the

MASSACHUSETTS INSTITUTE OF TECHNOLOGY

May 1987

©Elizabeth B. Welsh 1987

The author hereby grants to M.I.T. permission to reproduce and to
distribute copies of this thesis document in whole or in part.

Signature of Author

Department of Earth, Atmospheric and Planetary Sciences

Certified by

/

Nelson G. Hogg
Thesis Supervisor

Accepted by

/

W. F. Brace
Chairman, Department Graduate Committee

THE RELATIONSHIP OF TOPOGRAPHIC WAVES ON THE CONTINENTAL RISE TO GULF STREAM FLUCTUATIONS

by

Elizabeth B. Welsh

Submitted to the Department of Earth,
Atmospheric, and Planetary Sciences
on May 15, 1987 in partial fulfillment of the
requirements for the Degree of Master of Science in
Physical Oceanography

ABSTRACT

Current meter measurements from the Abyssal Circulation Experiment taken in the western North Atlantic on the Continental Rise and in the Gulf Stream are examined to determine horizontal and vertical structures of variable motions. Empirical orthogonal functions are used to examine characteristics of motions as a function of frequency. Waves in many low frequency bands exhibit properties of nearly barotropic topographic Rossby waves and are coherent over the ABCE array which includes a mooring within the Gulf Stream. Phase propagation of the waves is to the southwest indicating onshore energy propagation. Data from a second current meter array from the Synoptic Mapping experiment is examined to determine source region structure and relationship to Rise variability. In most frequency bands Stream motions are too complex to be separable in empirical modes but a significant mode exists in the band centered at a period of 30 days. Westward propagation is observed in the meridional component of the velocity and the associated zonal wavenumber matches that observed on the Rise. The hypothesis that westward propagating meanders can directly excite far field motions is examined and discussed.

ACKNOWLEDGEMENTS

I would like to thank Nelson Hogg for being an exceptional advisor, for his ideas and encouragement, and especially for being somewhat unique in recognizing that scientists aren't made in an aspic mold. Paola Rizzoli has also made numerous contributions and her enthusiasm and support has been appreciated, especially during the early years when positive feedback uncommon. The other members of my thesis committee, Nick Fofonoff and Jim Luyten, were generous with their time and their suggestions. Special thanks to Ross Hendry from Bedford Institute who selflessly allowed us the use of his data before having much of a chance to use it himself. Much appreciation goes to Rich Signell (I05.RPS1) for being a computer nerd so I didn't have to become one. And thanks to the MIT/WHOI Joint Program for allowing me to recognize my potential for neurosis so that I can more effectively guard against it in the future. This research was supported by ONR under contracts N00014-85-C-0001, NR 083-004, N00014-84-C-0134, NR 083-400, and N00014-82-C-0019, NR 083-004.

Contents

1	Deep variability in the western North Atlantic: a review	12
2	The ABCE Array	18
2.1	Time domain	22
2.2	Frequency domain	30
2.2.1	Vertical structure	31
2.2.2	Horizontal structure	37
2.3	Topographic Rossby waves: a review	47
3	Gulf Stream Variability	54
3.1	Time domain	54
3.2	Frequency domain analysis of the SME data	60
3.2.1	Vertical structure	63
3.2.2	Horizontal structure	65
3.3	Gulf Stream forcing of Rise motions	69
4	Discussion	80

List of Figures

2.1	Map of the western North Atlantic showing the ABCE and the SME current meter mooring arrays.	20
2.2	Schematic diagram of current meter moorings 775–780. . .	21
2.3	Temperature records at 500 meters and stick plots of current at moorings 775, 776, and 780	23
2.4	Stick plots of current with mean removed at moorings 775, 776, and 780.	26
2.5	Percent variance explained by the first three vertical modes at moorings 775, 776, and 780	32
2.6	Variance ellipse representation of vertical modes for moorings 775, 776, and 780 in the 120 day band.	34
2.7	Variance ellipse representation of vertical modes for moorings 775, 776, and 780 in the 30 day band.	35
2.8	Variance ellipse representation of vertical modes for moorings 775, 776, and 780 in the 17 day band.	36
2.9	Stick plot of current at the 500 meter level at mooring 776 with the Gulf Stream removed.	38
2.10	Current ellipse representation of vertical modes for mooring 776 with the Gulf Stream removed from the 500 meter record in three frequency bands.	39
2.11	Percent variance explained by the first three modes calculated from 4000 meter records from all six ABCE moorings.	40
2.12	Variance ellipse representation of deep horizontal modes in the 120 day band.	41
2.13	Variance ellipse representation of deep horizontal modes in the 30 day band.	42
2.14	Variance ellipse representation of deep horizontal modes in the 17 day band.	43

2.15	Phase propagation along and across isobaths in the 120, 30, and 17 day bands	44
2.16	Buoyancy frequency vs. depth taken from a CTD station made in June, 1983 and located at 60.5W, 39.5N	49
2.17	Dispersion relations for the near barotropic mode and vertical structures at three mooring sites in three frequency bands calculated from the model without mean flow included. . .	50
2.18	Dispersion relations and vertical structures at the three mooring sites in the three frequency bands as calculated from the model with mean flow included.	52
3.1	Temperature at 467 meters and stick plots at mooring 558.	56
3.2	Temperature at 445 meters and stick plots at mooring 557.	57
3.3	Temperature at 495 meters and stick plots at mooring 560.	58
3.4	Plot of sea surface temperature and inferred flow field on September 12, 1983.	61
3.5	Plot of sea surface temperature and inferred flow field on April 27, 1984.	62
3.6	Vertical structures of the first modes at moorings 561, 560, and 559 from the SME array.	64
3.7	Current ellipse representation of the horizontal 30 day mode calculated from Gulf Stream records from 4000 meters. . .	66
3.8	Phase plotted against distance east and north for u and v components from the first deep horizontal mode calculated from Gulf Stream records.	67
3.9	Phase plotted against distance along 24 degrees counter-clockwise of east. a. Gulf Stream mode. b. Rise mode. . . .	68
3.10	Vertical structures of the 30 day modes at mooring 780 for two segments of the record.	75
3.11	Percent variance explained by the first three modes calculated from the Stream and ring segments of the records on the Rise.	76
3.12	Variance ellipse representation of the Stream segment in the 30 day band.	77
3.13	Variance ellipse representation of the Stream segment in the 20 day band.	78

3.14 Time series of meridional component of velocity at moorings	
780, 561, 557, and 559.	79

List of Tables

2.1	The Abyssal Circulation Experiment array.	19
2.2	Coherence amplitudes calculated from the data series and the modal series from the vertical analyses at moorings 775, 776, and 780.	33
2.3	Coherence amplitudes calculated from the listed data series and the modal series from the horizontal analysis of 4000 meter records.	47
3.1	The Synoptic Mapping Experiment array.	55
3.2	Amplitudes, coherence values and phases from a mode constructed from all Rise records and the down- and cross-stream components from mooring 780-120 day band.	71
3.3	Modal amplitudes, coherence values and phases using down-stream and cross-stream coordinates from mooring 780-30 day band.	72
3.4	Modal amplitudes, coherence values and phases using down-stream and cross-stream coordinates from mooring 780-17 day band.	73
3.5	Coherence amplitudes between data series and modal series calculated from the Stream segments of the ABCE records.	74
3.6	Coherence amplitudes between data series and modal series calculated from the ring segments of the ABCE records.	74
4.1	Amplitudes, coherence values, and phases of velocity components associated with the first Gulf Stream 30 day mode constructed from all records from moorings 561, 557 and 559.	83

4.2	Amplitudes, coherence values, and phases of velocity components associated with the second Gulf Stream 30 day mode constructed from all records from moorings 561, 557 and 559.	84
4.3	Amplitudes, coherence values, and phases of velocity components associated with the 60 day horizontal mode including records from mooring 558.	86
4.4	Amplitudes, coherence values, and phases of velocity components associated with the 40 day horizontal mode including deep records from mooring 558.	87

Introduction

In the Abyssal Circulation Experiment (ABCE) current meter measurements were taken in a sparsely sampled region in the western North Atlantic from April 1983 until August 1984. The experiment was planned to better define the properties and boundaries of the larger of two recirculation gyres, the Northern Recirculation Gyre (NRG), found to exist in the available current meter measurements collected prior to 1983 (Hogg, 1983). The gyres as proposed in 1983 are shown in figure 2.1. In addition to the Worthington gyre to the south of the Gulf Stream, the eastward flowing branches of the two gyres contribute to the transport of the Stream, accounting for part of the difference between the observed transport and that which is predicted by wind driven circulation theory. A more detailed description of the experiment and a description of the mean properties of the NRG are presented in Hogg, Pickart, Hendry and Smethie (1985), and a model which is consistent with these findings is described in Hogg and Stommel (1985).

In the current records from the ABCE and other experiments conducted in the area, it is apparent that the near bottom flows on the Continental Rise and Slope are highly variable with standard deviations well in excess of the westward means causing very large instantaneous velocities to the west and flow reversals. These motions are so energetic that they have been called 'abyssal storms' or 'benthic storms' (Tucholke, Hollister, Biscaye, and Gardner 1985; Weatherly and Kelley, 1985). The causes of the storms are unknown, although a number of theories have been developed, many of which implicate Gulf Stream processes. Because the ABCE array samples both the Rise and the Gulf Stream, the data set is well suited for the investigation of this problem.

In addition, the Synoptic Mapping Experiment (SME), which was conducted by Ross Hendry from Bedford Institute in Nova Scotia, overlapped in time with the ABCE. In that experiment a current meter array was deployed in the Gulf Stream just to the east of the ABCE array. The first year of data collected in this experiment will be used in conjunction with the ABCE Stream mooring to examine Gulf Stream horizontal structure and its relationship to motions on the Rise.

The first chapter is a review of observations of deep variability and its possible causes as hypothesized by other researchers. Chapter 2 describes the results of both time and frequency domain analysis of the ABCE data. In chapter 3 a description of the SME data is given and is used in conjunction with the ABCE data to establish and explain a link between motions on the Rise and motions in the Gulf Stream. Finally, a discussion of the results of the data analysis follows in chapter 4.

Chapter 1

Deep variability in the western North Atlantic: a review

Much attention has been given the large amount of eddy energy on the Continental Rise and Slope of the western North Atlantic. A typical current meter record from the region shows superimposed on the mean flow nearly continuous low frequency variability most often associated with topographic waves, but sometimes associated with the deep signature of a Gulf Stream feature in a northern excursion.

It has rarely been possible to directly determine the sources of the waves on the Rise as the source regions have not often been sampled concurrently with the wave motions. Speculations have led to several theories, most of which suggest the involvement of Gulf Stream meanders and rings. Others are local mechanisms such as wind stress and destabilization of a mean flow over topography (Pedlosky 1980).

Louis and Smith (1982) concluded that wind stress could not explain the motions observed. Over a sloping bottom two wind stress terms appear in the potential vorticity equation constructed from the depth integrated momentum equations. The first is the familiar vertical component of the wind stress curl which might be important in the generation of very long topographic waves of basin length scales (Kroll, 1979). However, most of the length scales of the observed waves are $O(100 \text{ km})$. The second term is a coupling of the alongshore wind stress with the bottom slope, but Louis and Smith estimated that the amount of time needed to set up waves of the observed magnitude is too large.

Pedlosky (1980) examined the problem of instability of a mean flow with vertical and horizontal shear in a stratified fluid over a sloping bottom.

He found that if two conditions are met the flow can be destabilized and topographic waves can be generated. Two wave cycles 20 days in length were observed by Kelley and Weatherly (1985) at their 'shallow' mooring which is located very near mooring 775 of the ABCE array. They concluded that because there was no persistent Gulf Stream ring in the region to account for the wave energy, it was most likely that the mechanism proposed by Pedlosky was responsible for the burst of energy. They determined that the two conditions for instability were met at the site of the disturbance.

Other events observed by Kelley and Weatherly (1985) and Weatherly and Kelley (1985) are not topographic waves but are disturbances associated with the presence of the Gulf Stream over the mooring sites. This occurred at the deeper sites (called 'middle' and 'deep'). In these studies they show that the barotropic component of the meandering Stream or a ring often causes flow reversals and eastward bursts of energy at depth, and sometimes westward bursts of current. They attribute most westward bursts of energy to the restoration of the full strength of the westward current which is weakened or displaced to the north when a Gulf Stream feature is present at these mooring sites. This mechanism can only explain disturbances which occur in regions where Gulf Stream features frequently are present. It does not explain the majority of the energetic motions on the upper Rise and on the Continental Slope.

There is increasing evidence that the source of the observed motions is not local, but rather that the energy has propagated into the region from offshore. For example Hogg (1981) used a ray tracing technique on data from the Rise Array to locate the position of the source of observed topographic waves and found it to be in the vicinity of the Gulf Stream. Additionally, Thompson (1977) found the energy flux at site D to be directed shoreward. Johns and Watts (1986) also found a shoreward flux of energy associated with topographic waves observed off of Cape Hatteras at the location where the Gulf Stream leaves the Continental Rise. In response to these observational findings theories linking various Gulf Stream processes to far field motions have been developed to explain this transfer of energy.

In a study of the linear dynamics of Gulf Stream rings, Flierl (1977) concluded that much of the eddy energy surrounding the Stream system could be accounted for by dispersal of Rossby waves from baroclinic Gulf

Stream rings. In later numerical studies (McWilliams and Flierl, 1979) in which nonlinearities were included it was found that wave dispersal is a decreasing function of the nonlinearity of the vortex, and as Gulf Stream rings are highly nonlinear it was concluded that the rather slow dispersal of *baroclinic* Rossby waves from rings is insignificant. However, with the inclusion of nonlinear coupling between modes, they found that energy transfers to a barotropic mode occurred, apparently to achieve compensation in the lower layer (zero deep flow). Barotropic wave speeds are larger than baroclinic speeds and therefore barotropic dispersal could be significant in providing energy to the wave field.

To the north of the Gulf Stream system rings can propagate over sloping bottoms and Louis and Smith (1982) noted that an effect of an increasing slope is to increase the phase speed of Rossby waves. Eventually the phase speed may become large enough to linearize the dynamics and, as linearity enhances dispersal of Rossby waves, this process may account for the strong presence of topographic wave energy on the Continental Rise and Slope. They described the expected evolution of the radiation field and found the properties of bursts of topographic wave energy near the shelf break north of the ABCE region observed by Louis, Petrie, and Smith (1982) consistent with this theory. Slopes in the ABCE region are smaller than those under the moorings examined by Louis, Petrie and Smith and are not strong enough to linearize the dynamics of the rings, therefore if this mechanism were to drive motions at the more southern moorings of the ABCE array there must be a southward or offshore component to the direction of energy propagation. It will be demonstrated, however, that the flux of energy is shoreward for this data set (see Chapter 3).

Csanady explored a mechanism which might be responsible for transferring vorticity from a strongly surface intensified feature such as a meandering Gulf Stream or a ring to the deep ocean. Assuming nonlinear dynamics near the source and linear dynamics in the far field, and treating the nonlinear terms as sources for vorticity in each of two layers he found that the largest nonlinear term is a 'pressure torque' term which exists because there is a curl between the gradient vectors of surface displacement and interface displacement. He showed that a net transfer of vorticity from the upper to the lower layer occurs when a Gulf Stream ring is pinched off allowing for the generation of westward propagating Rossby waves or

topographic waves.

In addition to wave generation theories which implicate Gulf Stream rings, there are several hypotheses which suggest that the Stream itself might be a source for energy in the far field. One such mechanism is that of radiating instabilities from a jet which was examined by Lynne Talley in her doctoral thesis (Talley, 1982; also Talley 1983a, 1983b). As motions associated with the gravest unstable modes of an eastward jet would be trapped to within a few deformation radii of the current, they cannot account for strong disturbances far from the jet. Talley hypothesized that disturbances which grow more slowly, yet have larger trapping scales would dominate in the far field. These radiating modes were first explored by Dickinson and Clare (1973) in their examination of unstable modes associated with a hyperbolic tangent shear profile. The radiating modes look like Rossby waves in the far field with slowly decaying amplitudes away from the current. Talley explored these modes further in a linear model using a jet with both horizontal and vertical shear. The possibility for radiation exists if the phase speed for an unstable wave in the forcing region matches a phase speed for Rossby waves in the far field. By the semi-circle theorem phase speeds of unstable waves are within the range of the flow speeds, with a small correction for β . In practice Talley found that phase speeds for radiating modes are always within the range of flow speeds making it more difficult for an eastward jet to radiate than a westward jet. However, Talley found that under certain conditions radiation from an eastward jet can occur. Obviously, the conditions must allow the phase speeds of the Rossby waves and the unstable waves to overlap. Vertical shear in the far field will modify the potential vorticity gradient and may allow for positive phase speeds there. A westward undercurrent beneath the jet will expand the range of phase speeds to include negative values.

Talley's model assumed a flat basin and the question of how topography might affect the results arises, as the Stream often meanders over regions with large bottom slopes. Talley did study the effects of sidewalls and predicted that standing waves would be observed. However, some models of propagation of waves over the Continental Rise and Slope have indicated that refraction might be more important than reflection (Rhines, 1971, Louis and Smith, 1982). One might expect that the decay scales of the radiating modes will be affected by wave refraction. A separate question

concerns the effects that topography might have on the range of parameters allowed for radiation to occur. The enhanced β effect might be expected to inhibit the instability process and reduce the possibility of radiation.

Many researchers have examined the effects that a meandering Stream might have on the surrounding eddy field. Most studies have concentrated on the steady forced response of the ocean interior to meander forcing. In both linear (Pedlosky, 1977) and nonlinear (Malanotte-Rizzoli, 1984) studies of this type it was found that for Rossby waves to penetrate the ocean interior the phase speed of the meanders must be westward to match the free Rossby wave speeds. In more recent investigations which include the effects of a time dependent boundary, or growing and pulsating meander amplitudes, it was found that pulses of transient Rossby waves can radiate and become important far from the jet for both stationary and eastward propagating meanders in both the linear and the nonlinear cases (Malanotte-Rizzoli, Haidvogel, and Young, 1987; Malanotte-Rizzoli, Young, and Haidvogel, 1987). Radiation can occur provided that the frequency of the amplitude pulsations is below a critical frequency which is simply the upper bound on frequency for free waves in the interior.

Johns and Watts (1986) examined the possibility that topographic waves are associated with Gulf Stream meanders in data collected in a region near the location where the Stream leaves the coast, approximately 150 kilometers north of Cape Hatteras. This choice of locations allowed them to sample the envelope of the meanders and motions on the Rise with two moorings 30 kilometers apart. They used 3 current meters in the lower 2000 meters at each mooring and inverted echo sounders to measure the depth of the thermocline and hence the meanders of the Stream. It was concluded from frequency domain EOF analysis that topographic waves dominated in the lowest frequency band centered at a period of 32 days and meander related fluctuations dominated at higher frequencies.

To examine the relationship between the topographic waves and the surface meanders the coherence values between deep temperature records and thermocline displacements (as inferred from inverted echo sounders) were examined. Coherence values were low for the records from depths greater than 2000 meters in the 32 day band. They therefore concluded that the source of the waves was not local meandering of the Stream. However, the 32 day fluctuations which were compared to topographic wave theory

were found in the velocity records. For nearly barotropic fluctuations the temperature record may not be significantly coherent with the velocity records. This was found to be the case in waves in the ABCE data set. In fact, Johns and Watts did calculate coherence between cross-stream velocity and temperature and those values were found to be low in the lowest frequency band, especially at the deepest instruments. This result may be attributed to the more along bathymetry (15°) and therefore more along-stream (NE) orientation of the velocity. It would be informative to examine coherence between along-stream velocity and temperature to determine whether the latter can replace velocity as a signal for the observed topographic waves. They did note that the direction of energy propagation was onshore as it must be if generated by Gulf Stream disturbances and concluded that the source is downstream of their instrument array.

The models and observational results discussed in this chapter will be examined again in relation to the observational results from the ABCE and the SME data analyses in the following chapters.

Chapter 2

The ABCE Array

To gain better understanding of the dynamics of the Northern Recirculation Gyre (NRG), the Abyssal Circulation Experiment was conducted in the western North Atlantic during 1983 and 1984. The experiment yielded 17 months of current and temperature measurements over the full water column in a region which included the Gulf Stream and extended north to the Continental Rise. Table 2.1 lists the instruments, their locations, depths and lengths of operation.

Figure 2.1 shows the positions of the moorings of the array. The concentration of this work is on deep motions on the rise, and their relation to Gulf Stream variability. Consequently, only moorings 775–780 were used in the analyses. A schematic diagram of this segment of the array is shown in figure 2.2. Mooring 780 was in the Gulf Stream over much of the 17 month period. On occasion, the Stream meandered over moorings 776–779, so that these moorings were sometimes in, but most often north of the Gulf Stream. The Stream remained to the south of mooring 775 throughout the experiment.

Also shown in figure 2.1 is the NRG as proposed by Hogg in 1983. Moorings 775–779 were located in the northern branch of the NRG and therefore these records show relatively strong deep mean flows to the southwest following bottom contours. The mean flow at mooring 780 is to the east at all levels. A thorough description of the mean fields is given in Hogg, Pickart, Hendry, and Smethie (1985).

Inst.	Start Date	# Days	Depth (m)	Water Depth	Lat.	Long.
7751	3-20-83	506	497	4027	41.20	-63.02
7752	3-20-83	506	1390	4027	41.20	-63.02
7753	3-20-83	424	3987	4027	41.20	-63.02
7762	3-20-83	507	518	4886	40.48	-62.06
7764	3-20-83	507	1512	4886	40.48	-62.06
7765	3-20-83	507	4011	4886	40.48	-62.06
7766	3-20-83	507	4789	4886	40.48	-62.06
7771	3-21-83	506	4002	4970	40.21	-61.59
7772	3-21-83	506	4871	4970	40.21	-61.59
7781	3-21-83	523	4002	4760	40.68	-61.50
7791	3-22-83	506	4005	4798	40.94	-60.72
7802	3-22-83	507	513	5140	39.48	-60.33
7804	3-22-83	507	1009	5140	39.48	-60.33
7805	3-22-83	507	1506	5140	39.48	-60.33
7806	3-22-83	507	4004	5140	39.48	-60.33

Table 2.1: The Abyssal Circulation Experiment array.

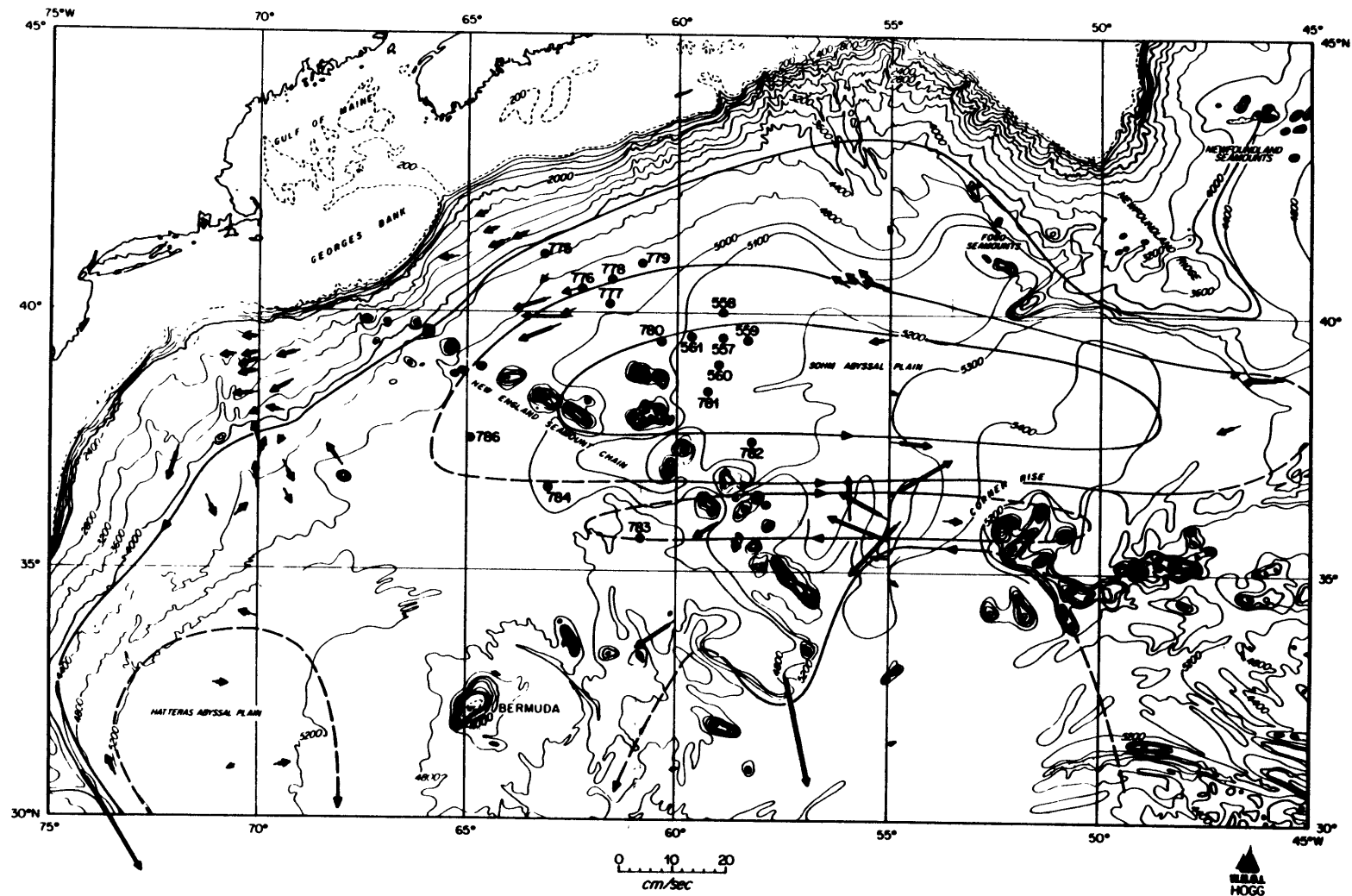


Figure 2.1: Map of the western North Atlantic showing the ABCE (775-786) and the SME (557-561) current meter mooring arrays. From Hogg (1983).

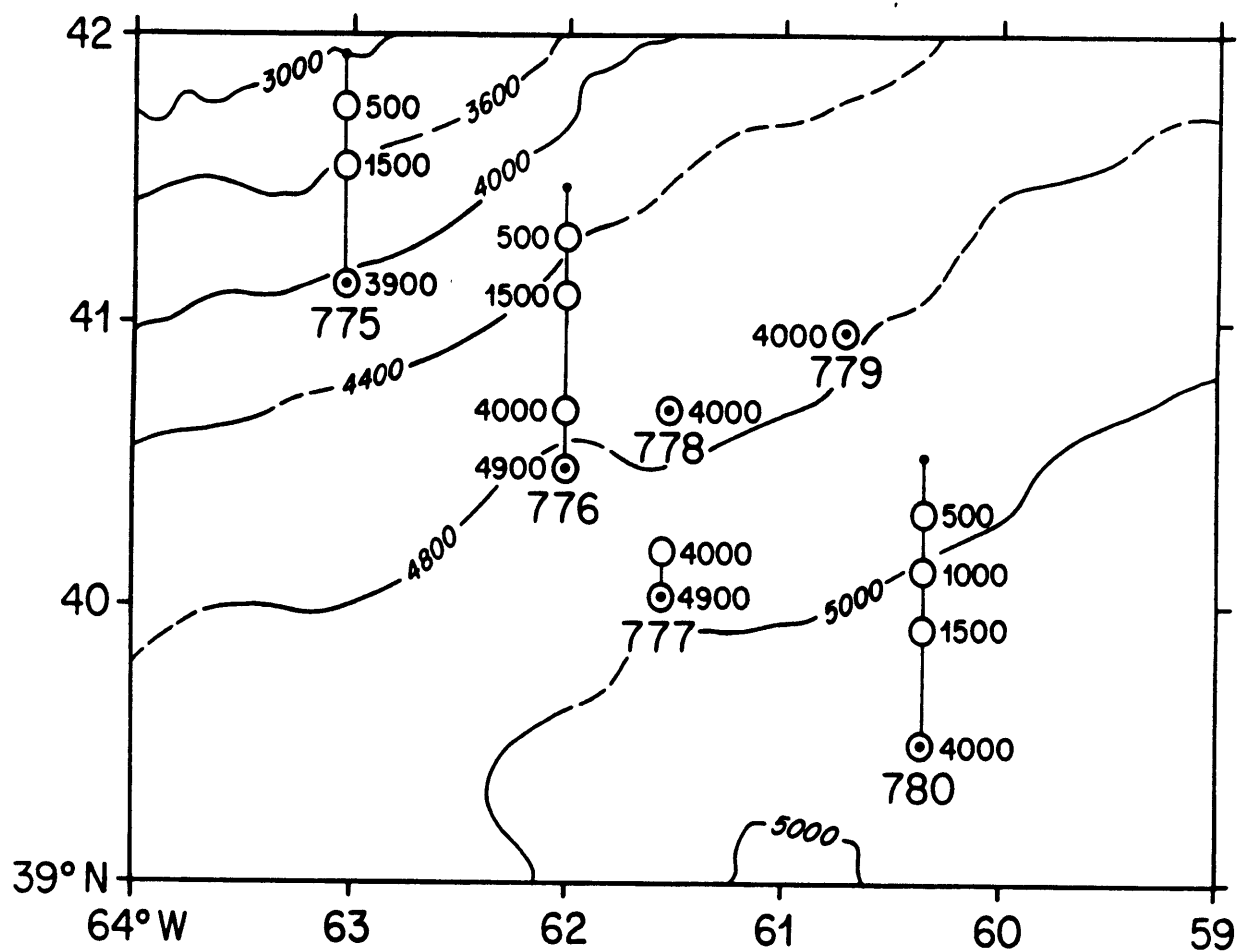


Figure 2.2: Schematic diagram showing the positions and depths (in meters) of instruments on moorings 775-780 from the ABCE array.

2.1 Time domain

Stick plots of current vectors and time series of temperature at three of the moorings are shown in figure 2.3. Warmer temperatures and eastward flow at 500 meters are indicative of the presence of a Gulf Stream feature. Mooring 780 was clearly in the Stream for much of the 17 months. Flows are strong, to the east and surface intensified. The Stream appears to extend coherently to the bottom, although the current at the deep instrument level is smaller in magnitude. This coherence is consistent with the findings from a mooring near 68°W of Hall and Bryden (1985).

Motions at mooring 775, are usually to the west at all depths and there is evidence of bottom trapping. In fact, motions are not as clearly related to those at the upper level instruments as they are at moorings 776 and 780. Events at 4000 meters are of comparable magnitude to those at the same depth under the Gulf Stream (as high as 30 cm s^{-1}). In addition, there are a significant number of flow reversals which occur most often at the 4000 meter level.

The most complex motions are found in the vicinity of mooring 776. The bottom records show two types of disturbances. The first type is associated with eastward bursts of current at 500 meters accompanied by temperatures which are well above the mean. These fluctuations extend throughout the water column usually reversing the flow at the 4000 meter instrument. The second type of motion is barotropic or slightly bottom intensified. These motions are not associated with an overlying Gulf Stream feature as there is no corresponding temperature disturbance at 500 meters. When the mean is removed from the records (fig. 2.4), the Gulf Stream related fluctuations are still surface intensified, but are nearly constant in amplitude at instruments below 500 meters. The second type of feature still appears to be barotropic, and these fluctuations are of comparable magnitude to those directly forced by the Stream. The bottom record with the mean subtracted is not clearly dominated by either type of fluctuation.

As mentioned in chapter 1, one theory for the existence of high levels of deep energy was presented by Weatherly and Kelley (1985). They used satellite data from the National Weather Service to determine the position of the Gulf Stream, in conjunction with records from deep current meters. By defining an event to be the persistence of flow in excess of 15 cm s^{-1}

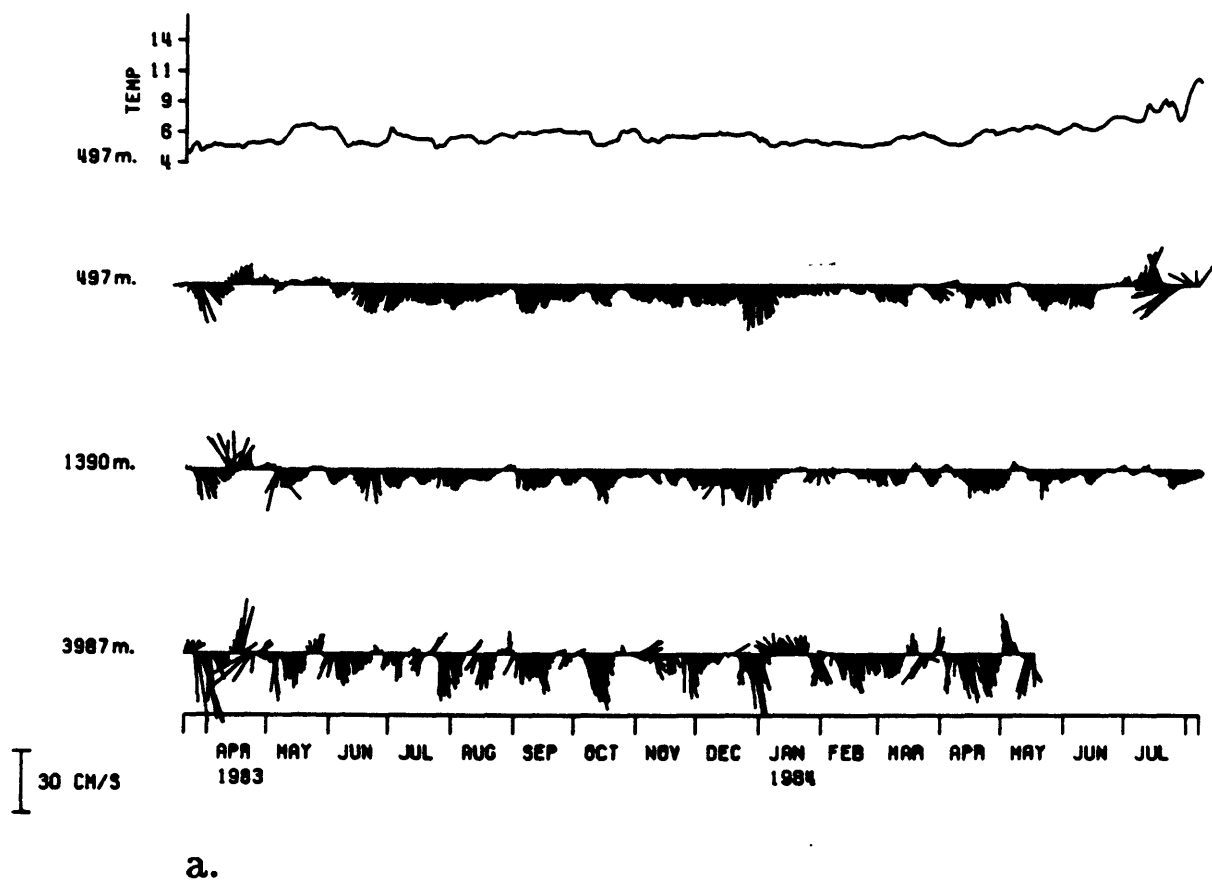
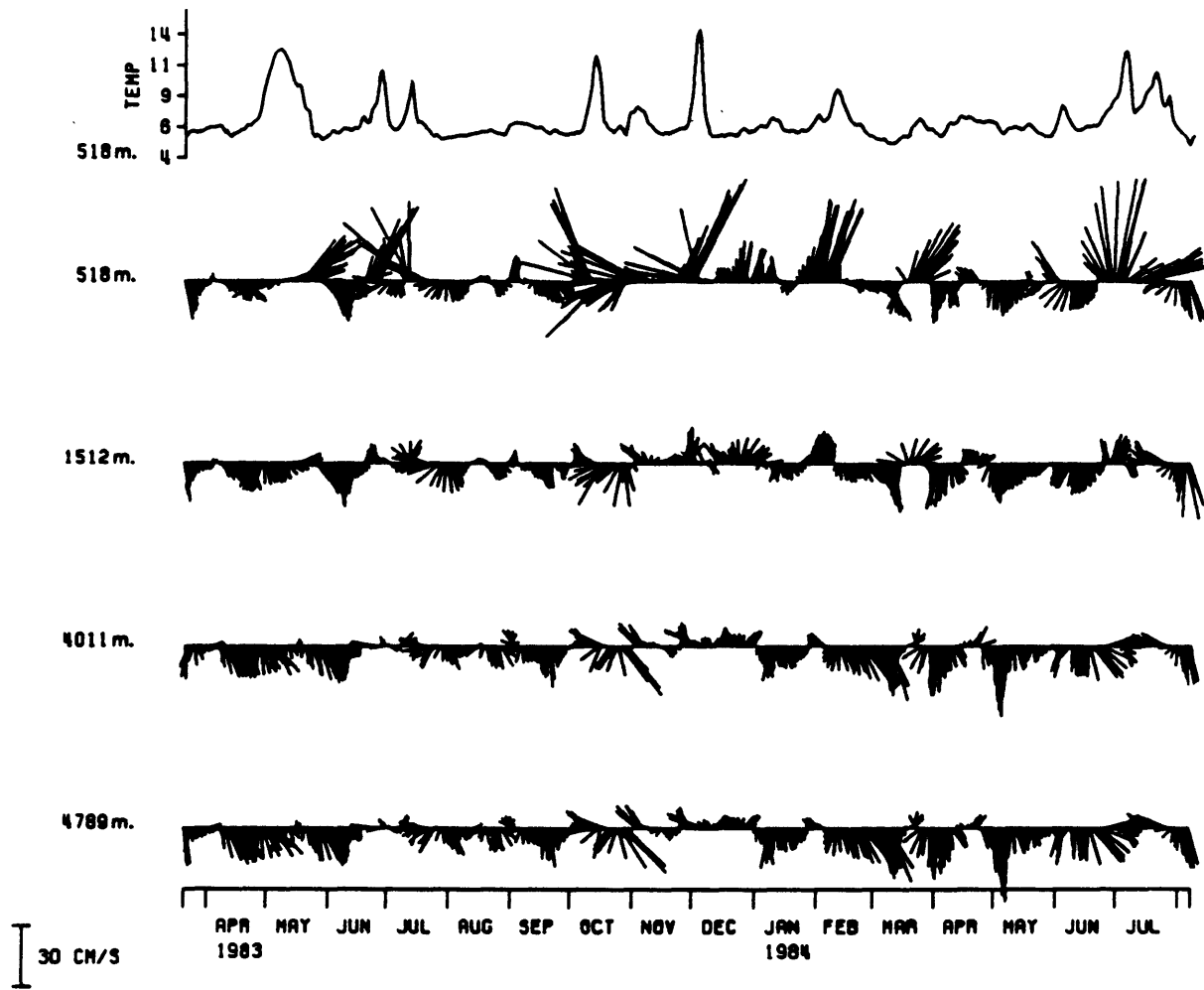
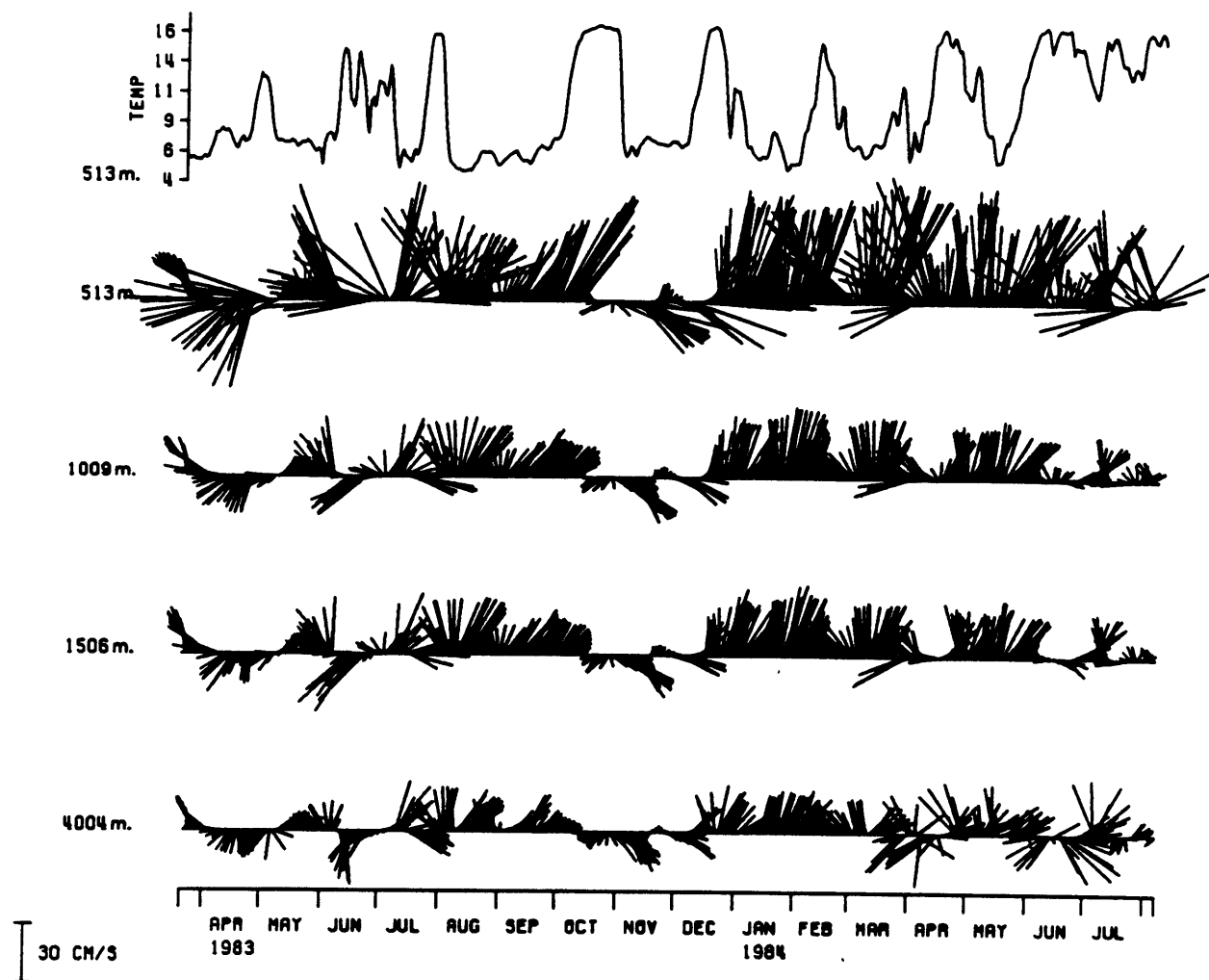


Figure 2.3: a. Temperature records at 500 meters and stick plots of current at mooring 775. b. Mooring 776. c. Mooring 780. East is up.



b.



C.

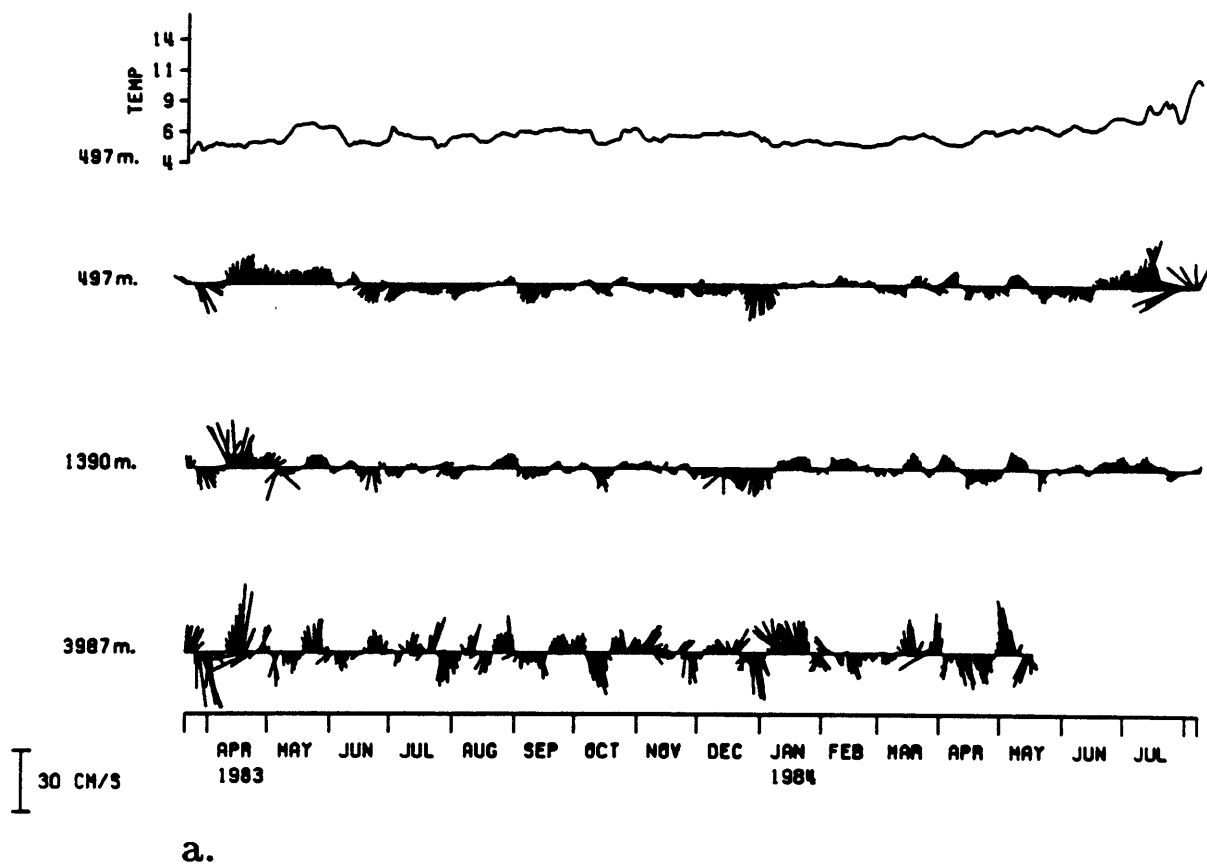
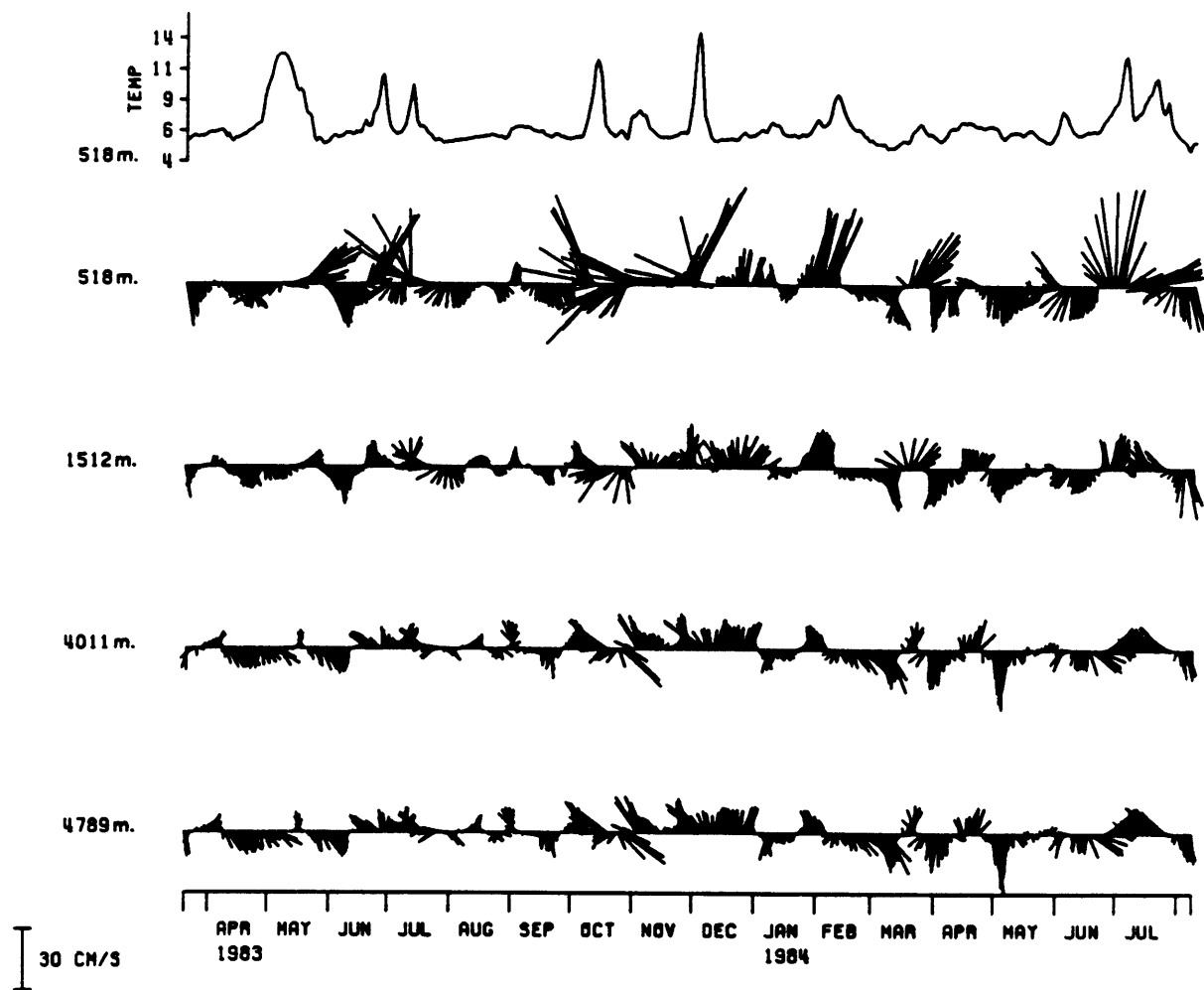
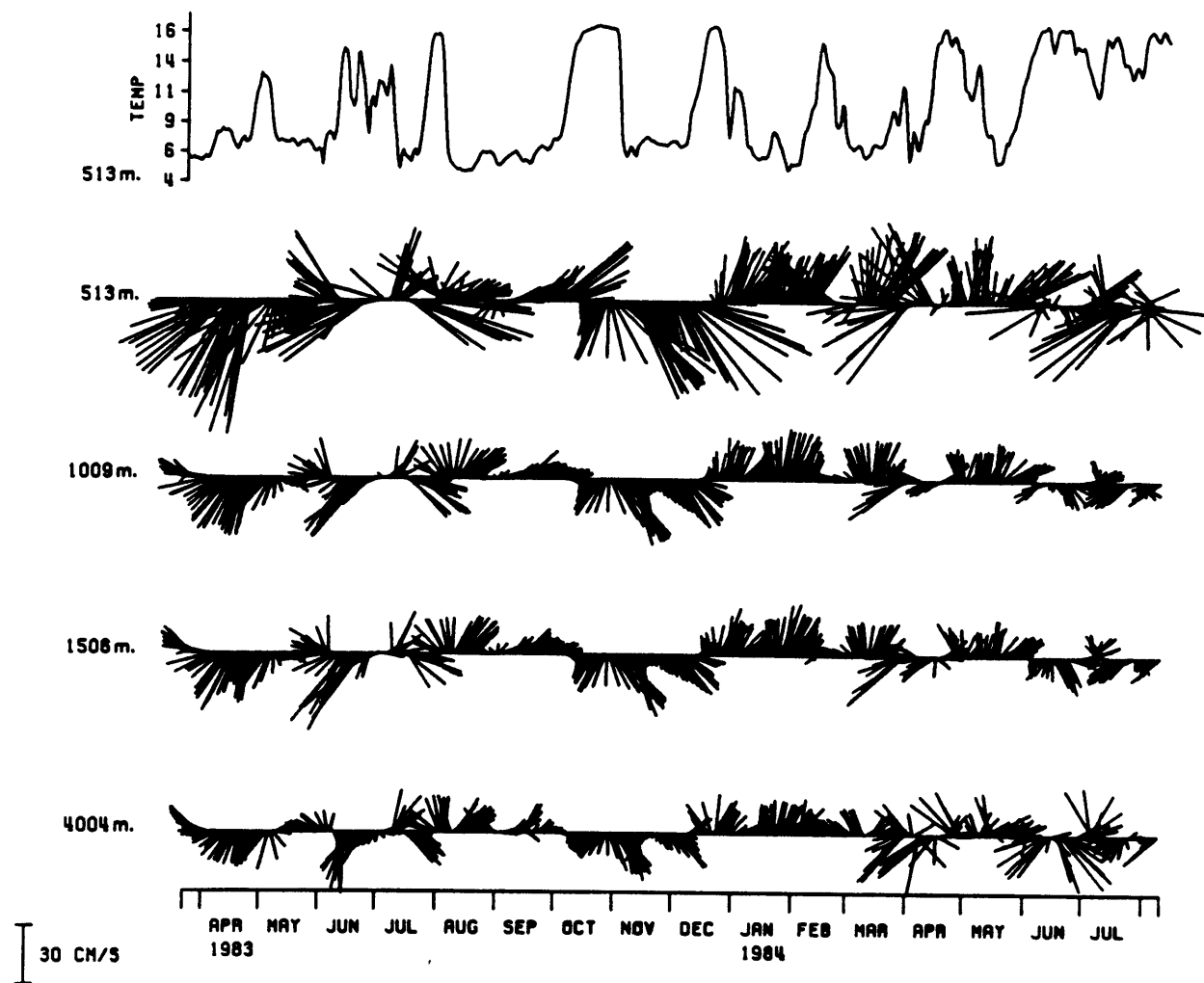


Figure 2.4: Stick plots of current with mean removed at moorings a. 775, b. 776, and c. 780. The original temperature series at 500 meters are also shown.



b.



C.

for 2 or more consecutive days they found that most of the relatively few eastward events could be explained by a meander or the northern side of a ring which extended to the bottom reversing the flow. Only a few of the westward events could be accounted for by the presence of the southern part of a Gulf Stream ring overhead. To explain the remaining events they argued that the Cold Filament Current (CFC), which is the near bottom manifestation of the westward flowing branch of the NRG, is strong enough to account for the remaining events. When the Stream or a ring is overhead the barotropic component of the feature will extend to the bottom causing a reduction in amplitude or displacement of the westward current. When the Stream is *not* over the mooring, the CFC can regain its full strength and an apparent 'burst' of energy occurs.

Because the data from the ABCE includes temperature records at 500 meters, the presence of a Stream feature at the mooring site can be more accurately observed, since the surface temperature front given by the satellite data is often in a different position than the subsurface front (Weatherly and Kelley, 1985). The temperature at 500 meters at mooring 776 exceeds the mean temperature for roughly 30 percent of the record. During these times the deep fluctuations can be accounted for by the presence of the features over the mooring. However the assertion that the resumed strength of the CFC can account for the remaining bursts of deep energy cannot be demonstrated with this data set for a number of reasons. First, if the theory of Weatherly and Kelley could explain the deep variability then approximately 70 percent of the record should show the strong westward flow of the CFC with relatively less variability. However, the flow is as variable during these parts of the record, including a comparable number of strong events. Second, the mean of the zonal component of velocity when the effects of the Gulf Stream are removed can be estimated by removing days where the temperature at 500 meters exceeds the mean temperature. This value is approximately -7.5 cm s^{-1} . This might be a slight underestimate of the actual value, but the value necessary to support the hypothesis of Weatherly and Kelley was -15 cm s^{-1} , or twice the value estimated here. The bursts of current are typically -15 to -20 cm s^{-1} , and sometimes have magnitudes of -35 cm s^{-1} and therefore cannot be attributed to a current of the estimated magnitude. Finally, in the next section, it will be demonstrated that the bottom motions at this mooring are coherent with those at

the other moorings in the array, including mooring 775 which is out of range of the Stream, suggesting that the forcing mechanism affects the flow over a much larger scale than would be expected if the mechanism suggested by Weatherly and Kelley were responsible for the deep variability.

2.2 Frequency domain

Empirical orthogonal functions can be an effective means of describing large amounts of data, if most records are sufficiently coherent and dominated by one or two processes. In the portion of the ABCE array used in this study there were 15 current meters, each with measurements of temperature and two components of velocity. Therefore this method was considered to be the most reasonable choice for the data analysis. For a thorough description of empirical orthogonal functions, refer to Wallace and Dickinson (1972). A short description is given here.

In EOF analysis in the time domain the covariance matrix is formed from all available time series, and the eigenvalues (λ_i) and the eigenvectors (e_{ij}) are determined. A set of orthogonal functions are constructed, each of which are combinations of the input time series. The i^{th} modal series is given by the expression

$$z_i(t) = \sum_j e_{ij} u_j(t).$$

The eigenvalues of the matrix are real and can be ordered— the i^{th} eigenvalue of the matrix reveals the variance explained by the i^{th} empirical mode. If a large fraction of the variance is explained by the first few modes, then the physical properties present in the data set can be concisely described by these relatively few time series, and the corresponding eigenvalues and eigenvectors.

Wallace and Dickinson outline a similar method of computing empirical orthogonal modes in the frequency domain, which gives information about time scales and phase relationships between contributing series. Because the interest in this study is on the variability and not the mean fields, this method was used.

In the frequency domain analysis the modal series is

$$z_i(t) = \Re \sum_j e_{ij} w_j(t)$$

where

$$w_j(t) = [u_j^f(t) - i\omega^{-1} du_j^f(t)/dt]$$

in which u_j^f is a filtered time series obtained by removing all spectral components outside the desired frequency interval. In this case the e_{ij} are the complex eigenvectors of the cospectral matrix. As in the time domain, the functions are orthogonal and the eigenvalues are real. In practice the coherence matrix is often used to prevent the modes from being dominated by the input series with the highest dimensional values.

The determination of the modes is simply the first step as it, by itself, gives no information about the physical processes involved. According to Wallace and Dickinson, if the first eigenvalue is large compared with the second, there is probably one dominant wave type present in the data. If, however, the first two modes explain comparable amounts of the variance in the data, then probably two or more wave types are present which are not necessarily orthogonal. In the latter case comparison to physical models is difficult. A second consideration is how many individual time series contribute significantly to the mode. To determine this, the coherence between the z_i series and each data series must be calculated, and if the important contributors are spatially random, then the physical significance should be questioned.

2.2.1 Vertical structure

The method of empirical orthogonal functions was first used to examine the vertical structure at moorings 775, 776, and 780. Initially, the modes were calculated for each mooring separately and consequently the structures found may not be related to those at other moorings. Temperature values were reduced to 10% of their real values in the determination of the coherence matrix. This downweighting of temperature allows for a more accurate description of the current variability. However, after the modal series were determined the coherence of the original temperature records with the modal series was calculated to determine whether or not the temperature records are also related to the velocity modes.

Figure 2.5 shows the percent variance explained as a function of frequency by each of the first three modes for each mooring. At all three moorings a significant first mode appears in the 120 day band, the 30 day

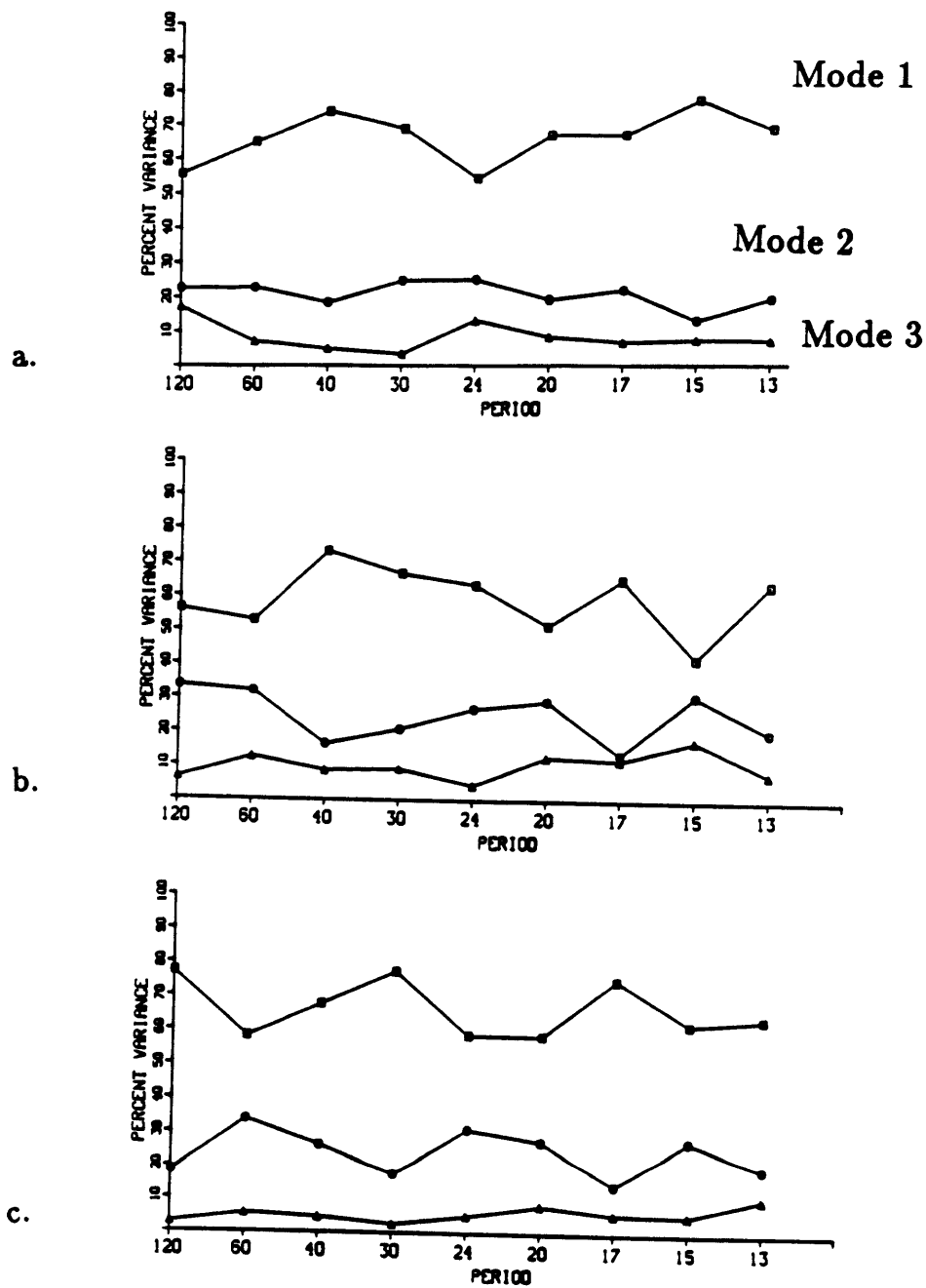


Figure 2.5: Percent variance explained by the first three vertical modes at moorings a. 775, b. 776 and c. 780. Temperature was downweighted in the determination of the modes (see text).

Inst.	120 days		30 days		17 days	
	coh <i>u</i>	coh <i>v</i>	coh <i>u</i>	coh <i>v</i>	coh <i>u</i>	coh <i>v</i>
7751	63	61	73	88	84	70
7752	91	78	86	93	87	84
7753	88	77	92	90	93	88
7762	80	59	78	81	82	84
7764	81	81	83	92	83	84
7765	92	93	88	86	77	79
7766	94	90	89	85	79	75
7802	83	83	80	88	90	82
7804	82	85	90	89	88	92
7805	80	82	90	88	88	93
7806	76	82	94	85	82	82

Table 2.2: Coherence amplitudes calculated from the listed data series and the modal series from the vertical analyses at moorings 775, 776, and 780. An amplitude of 62 is significant at the 95 percent confidence level.

band , and the 17 day band and these bands will be more thoroughly described, giving information about motions in a broad range of time scales.

Table 2.2 gives the coherence amplitudes between velocity series and modal series in the three bands. Values are high throughout the water column at each mooring site and in each frequency band. This is especially of interest in relation to the Gulf Stream mooring, 780. The features described by the modes extend coherently to the bottom.

The amplitude of the individual time series explained by the mode is given by $coh \cdot \sqrt{\Delta\omega \cdot \sigma^2}$, where $\Delta\omega$ is the frequency interval, σ^2 is the spectral density of the series in that frequency band, and coh is the coherence amplitude between the data record and the modal series. Current ellipses calculated from modal *u* and *v* amplitudes and relative phases were superposed on the bathymetry and are shown in figures 2.6–2.8. Horizontal displacements of the centers of the ellipses represent vertical phase shifts of the major axis component of the velocity. In calculating ellipses, it is necessary to have coherence between both components of velocity and the modal

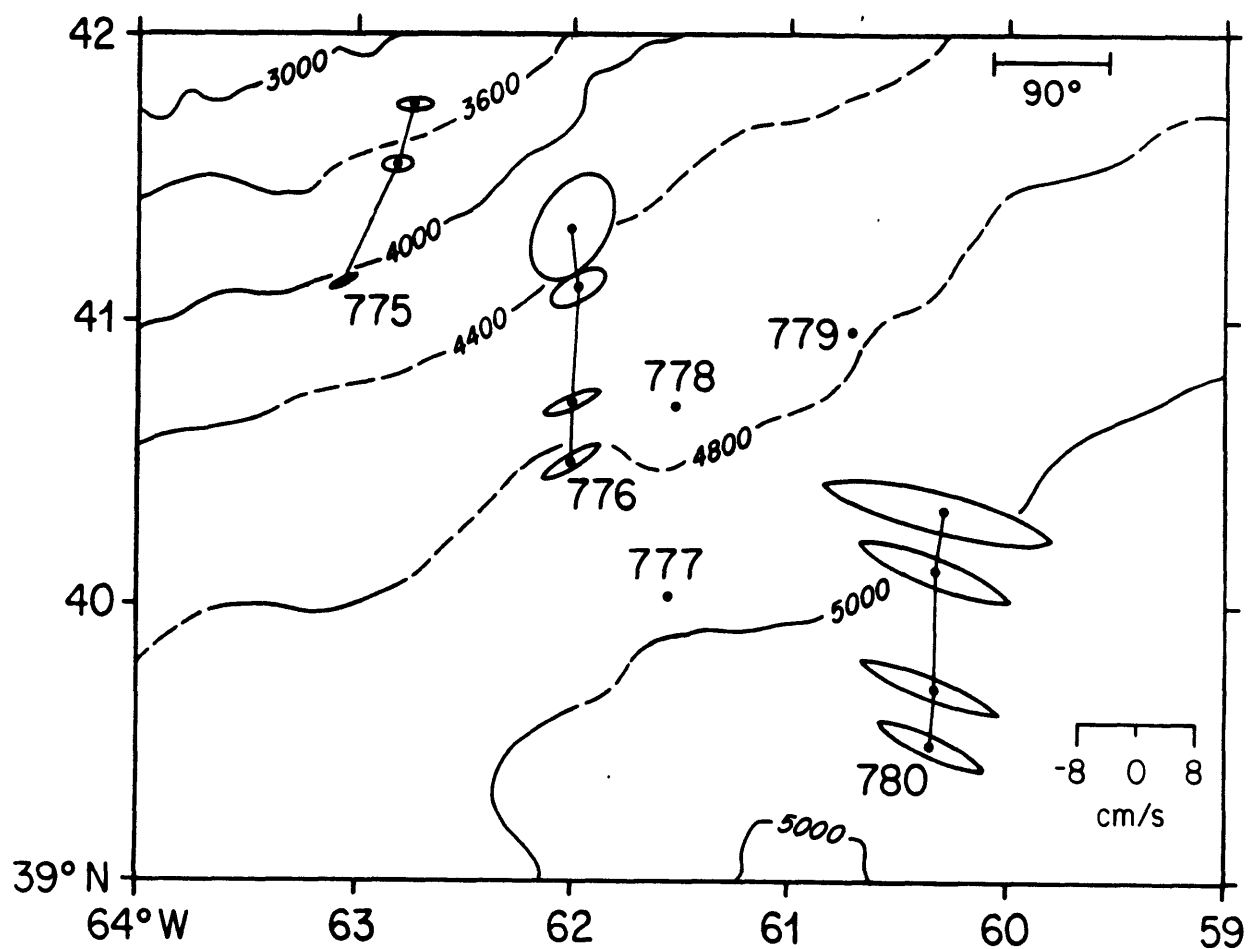


Figure 2.6: Variance ellipse representation of vertical modes for moorings 775, 776, and 780 in the 120 day band. Horizontal displacements of centers of ellipses represent vertical phase shifts of the major axis component of velocity.

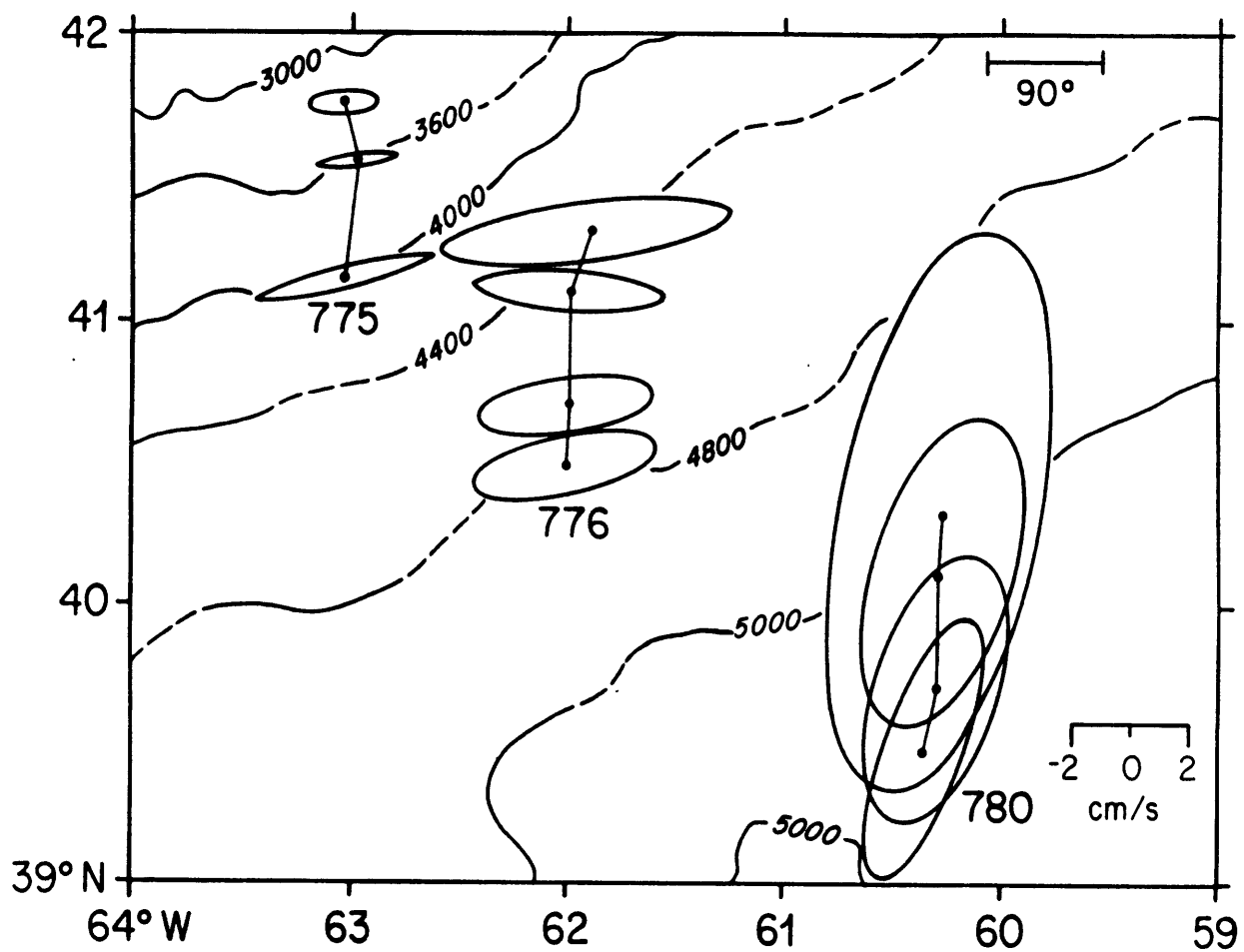


Figure 2.7: As in fig. 2.6 in the 30 day band.

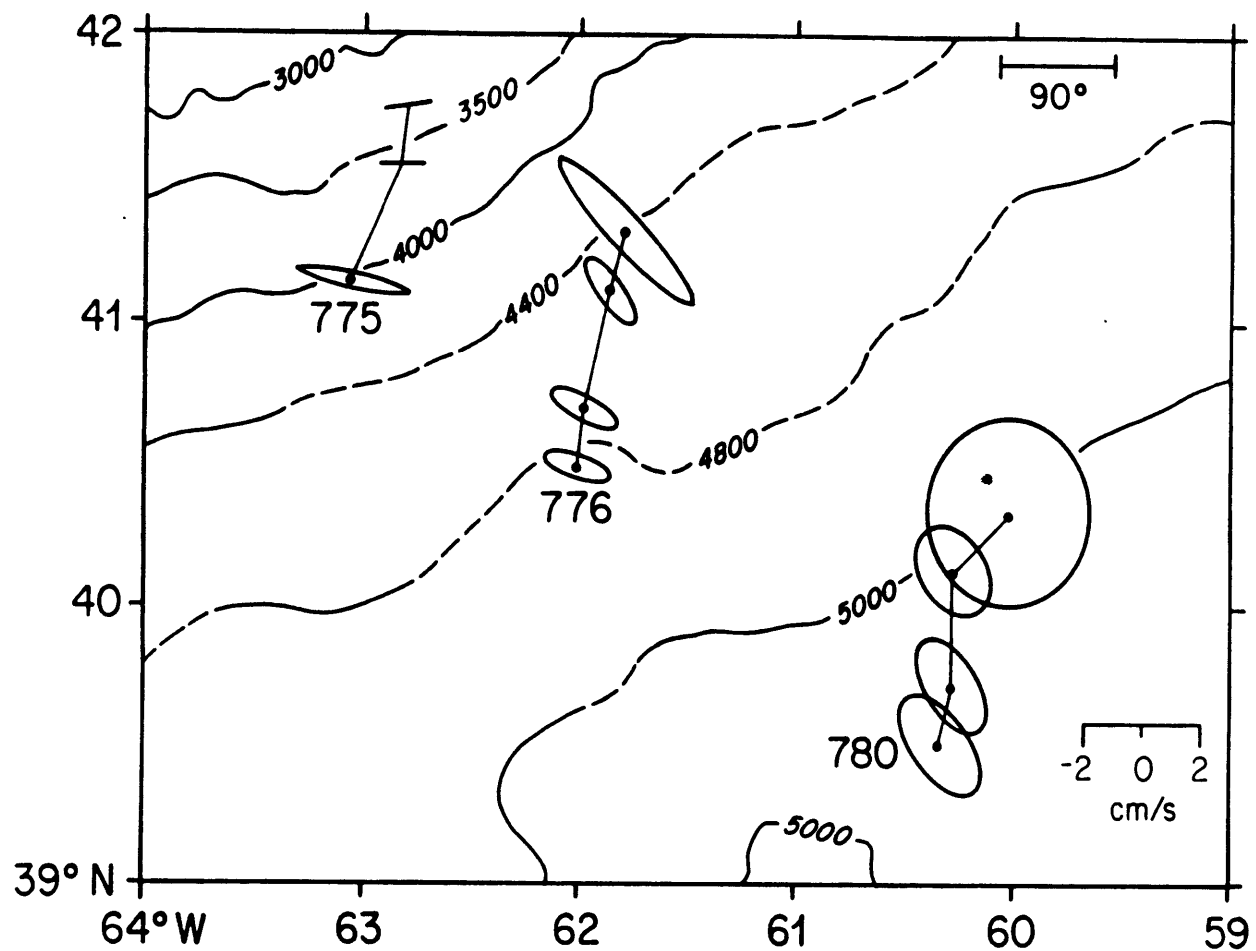


Figure 2.8: As in fig. 2.6 in the 17 day band.

series to get reliable estimates of phase. Because orientations of motions vary with frequency, different coordinate systems were used for each band. The aim was to find a coordinate system in which equal amounts of variance are present in both velocity components. Thus a coordinate system which makes an angle of 45 degrees with the direction of the orientation of the ellipse is optimal. The coordinate systems used in all analyses of the 120, 30 and 17 day bands are 64, 41, and 24 degrees counterclockwise of east respectively.

At mooring 775 the modes show that the energy is trapped near the bottom. At moorings 776 and 780 the amplitudes are quite constant with depth except at 500 meters, where the amplitudes are significantly larger. This can be attributed to the presence of a surface intensified Gulf Stream at each of these moorings. This should have a significant effect on modal structure at mooring 780 as motions there are dominated by Stream activity. At mooring 776 it is unclear whether the observed mode explains primarily those disturbances that exist when the Stream is over the mooring, or if a significant part of the mode consists of the barotropic motions which were also observed at this mooring and described in section 2.1.

To examine this question, an attempt was made to remove the influence of the Gulf Stream from the 500 meter record. On 145 out of 507 days the temperature at that level exceeded the mean temperature for the record. On these days the values of the velocity components and the temperature were replaced by their mean values. The resulting velocity series is shown in fig. 2.9. The altered series were then used to calculate a new mode. The coherence of the altered series with the recalculated mode was reduced in all frequency bands, but was still significant. The resulting modal ellipses are shown in figure 2.10. The new amplitudes are nearly constant with depth. This appears to indicate that the modes in these frequency bands are composed both of motions associated with a surface Gulf Stream, and those barotropic motions which exist when the Stream is absent from the site of mooring 776.

2.2.2 Horizontal structure

To facilitate understanding of driving mechanisms of deep flows on the rise, it is also necessary to determine their horizontal structures. Therefore, the

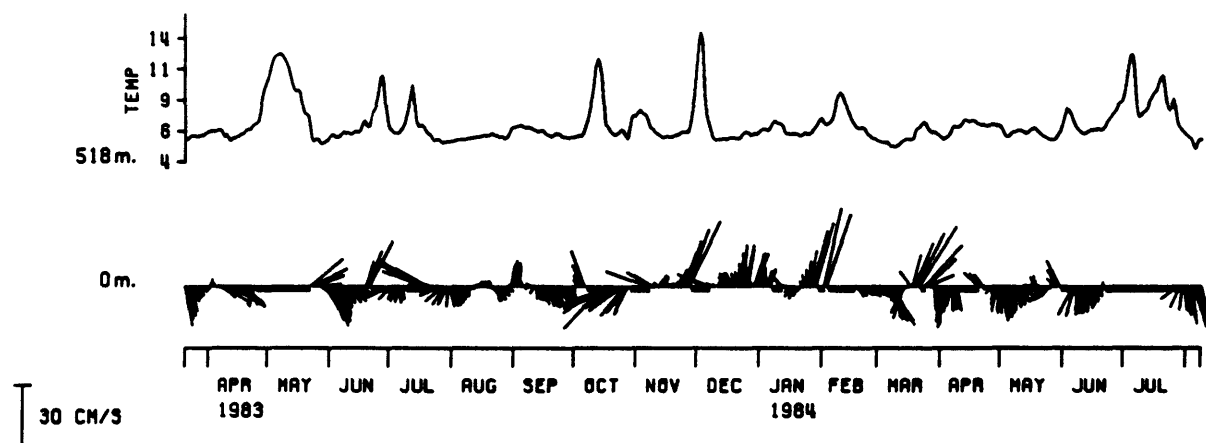


Figure 2.9: Stick plot of current at the 500 meter level at mooring 776 with the Gulf Stream removed. The original temperature series is also shown.

4000 meter records from all moorings were used to calculate deep empirical modes. Figure 2.11 shows the percent variance as a function of frequency explained by the first three modes. As in the vertical analyses, temperature was downweighted in the calculation of the coherence matrix, so that the descriptions are again of current variability.

A notable feature in the percent variance plot is the absence of significant modes at 13 and 15 days. Referring back to figure 2.5 shows that significant modes appear in these bands at all three moorings except in the 15 day band at mooring 776. This reduction in significance in the horizontal analysis is an indication that the driving of these motions may be a more local process. Kelley and Weatherly (1984) determined that the two conditions for instability over topography were met at the location of their 'shallow' instrument which is very close to the position of mooring 775 in this study. Possibly this destabilization mechanism is responsible for these motions at mooring 775. At moorings 776 and 780 direct Gulf Stream forcing might excite motions in these bands.

In the remaining bands first modes tend to be more significant suggesting that larger scale process may dominate motions at lower frequencies. Significant modes exist in the three bands centered at 120, 30, and 17 days and these bands will again be described. Figures 2.12–2.14 show the ellipses

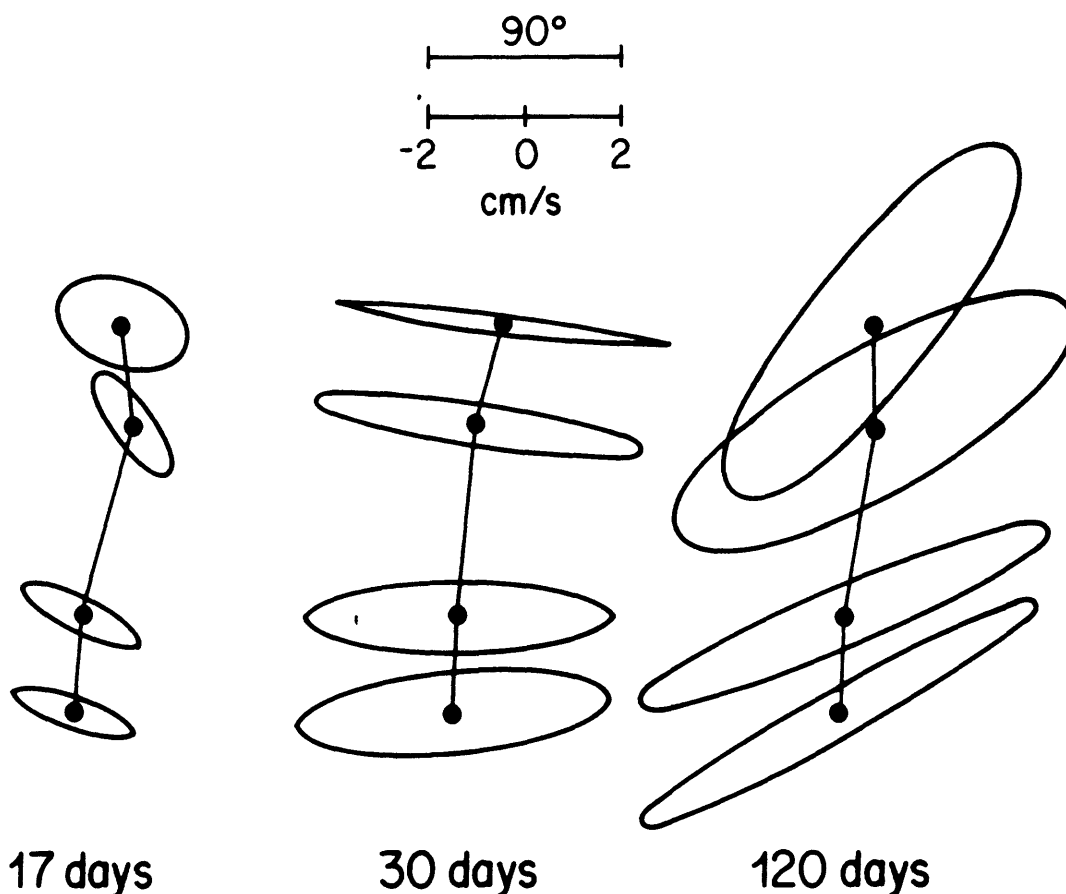


Figure 2.10: Current ellipse representation of vertical modes for mooring 776 with the Gulf Stream removed from the 500 meter record in three frequency bands.

calculated from the first mode in each band. Table 2.3 indicates which series are significantly coherent with the modes in the three bands. The amount of coherence is somewhat dependent upon the variability of direction of the current over the array since the coordinate system used is the same for each location (section 2.2.1). For example, in the 120 day band, the orientations of the ellipses are quite uniform over the array and all series are coherent except those at mooring 775 where neither component is coherent with the mode. Therefore the choice of a coordinate system was appropriate at all locations. However, the orientations of the ellipses change significantly in the 17 day band, possibly responding to local topographic features, and the choice of coordinate system is not uniformly

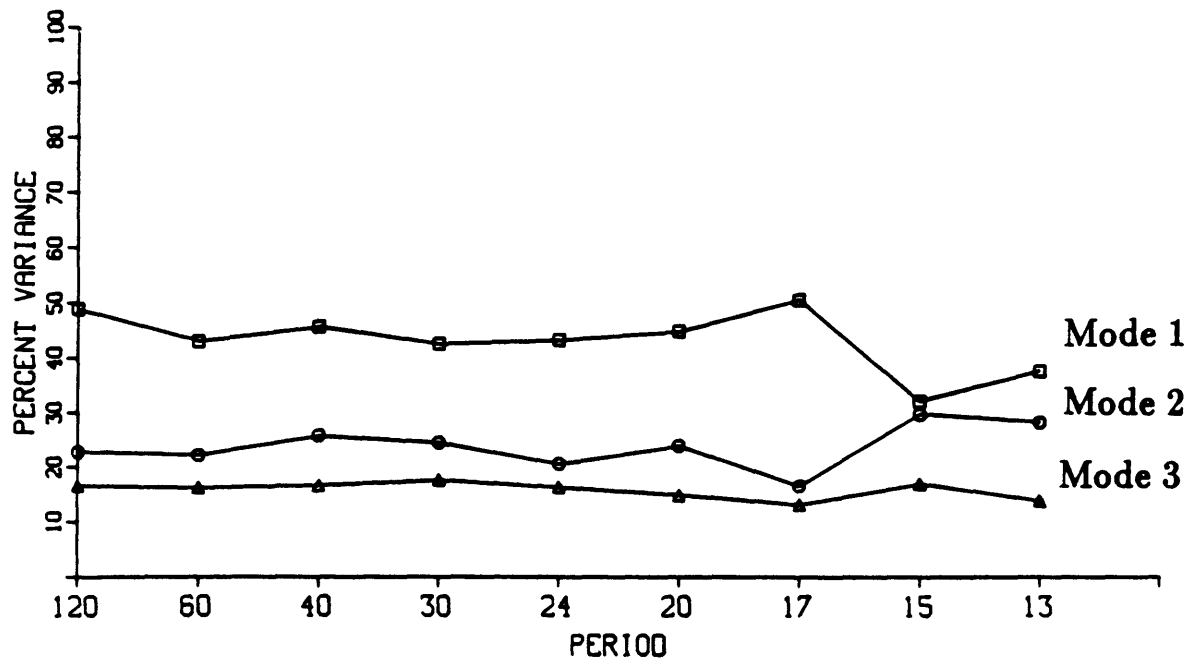


Figure 2.11: Percent variance explained by the first three modes calculated from 4000 meter records from all six ABCE moorings.

optimal. Even in this band, however, most time series are coherent with the mode. The orientations and amplitudes at moorings 775, 776, and 780 are similar to those found in the vertical analysis at the 4000 meter level, suggesting that these horizontal modes have the vertical structure previously described. Some interesting findings are the apparent relationship between the motions on the Rise with the motions at the Gulf Stream mooring, 780, and the near uniformity of the amplitude of the motions over the array.

Figure 2.15 illustrates phase propagation of the observed waves. Phase is plotted against distance along and across isobaths in each of the three frequency bands, and for each input velocity component. Because bottom slope changes over the array, and becomes quite significant at mooring 775, a linear relationship between phase and distance 'north' should not

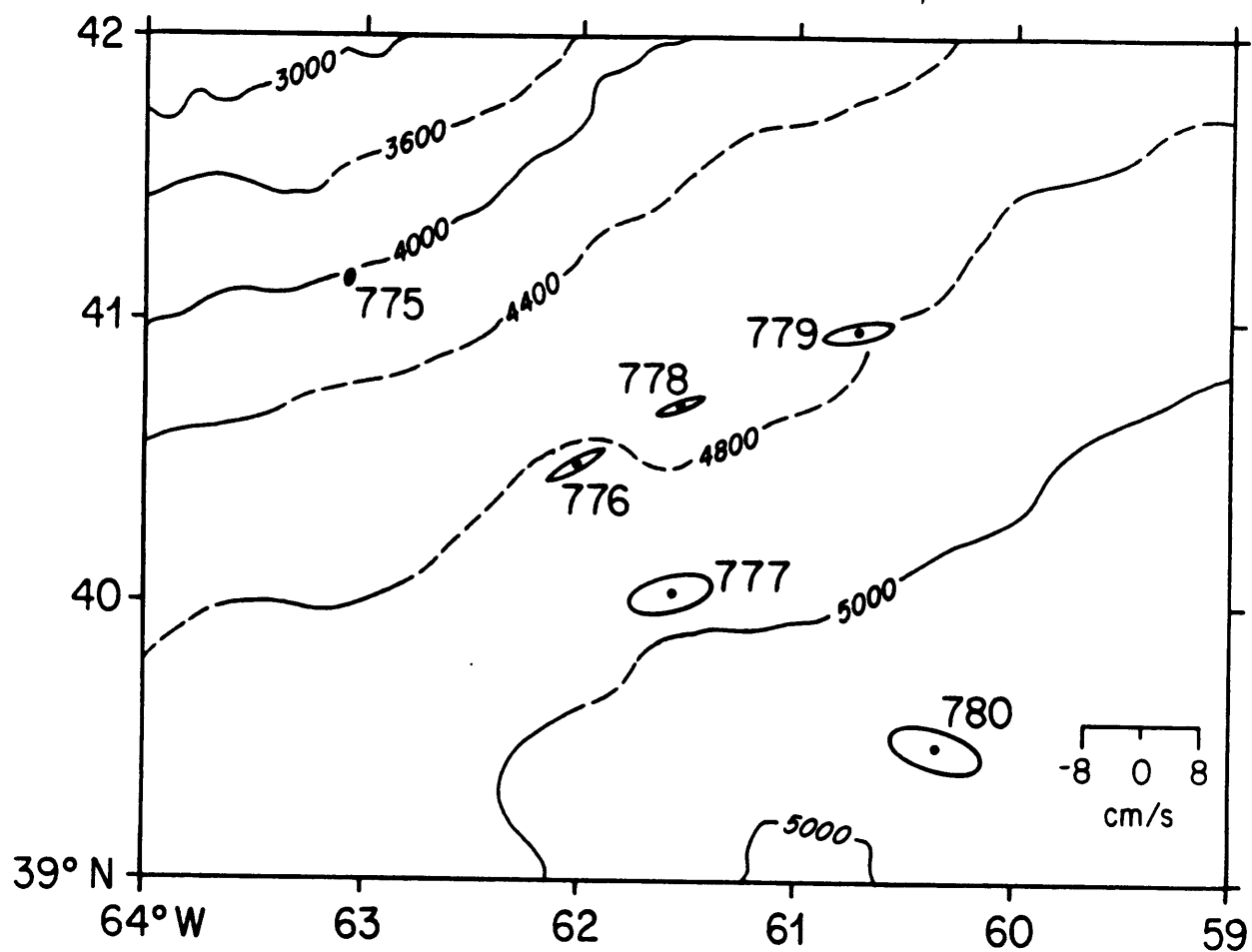


Figure 2.12: Variance ellipse representation of deep horizontal modes in the 120 day band.

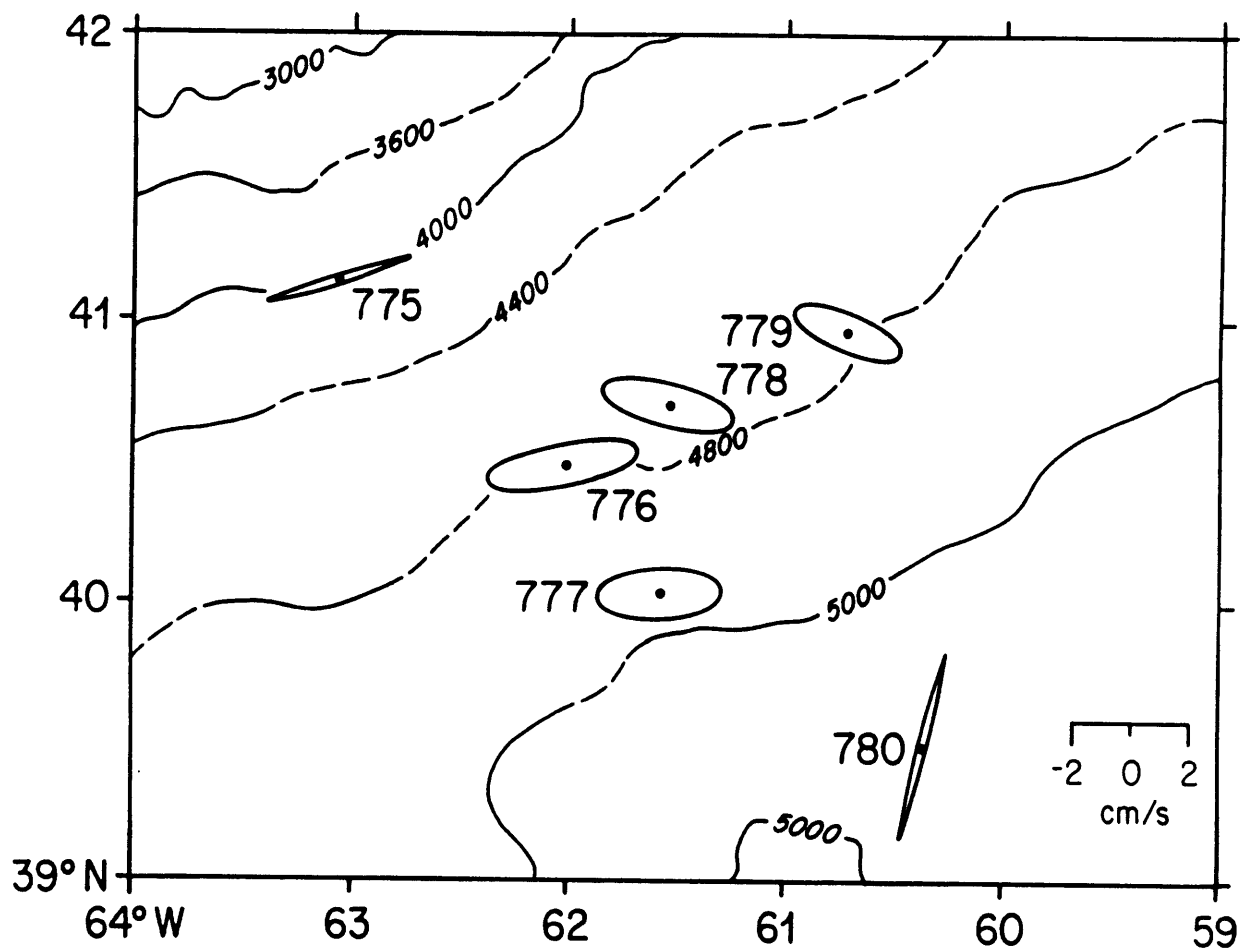


Figure 2.13: Variance ellipse representation of deep horizontal modes in the 30 day band.

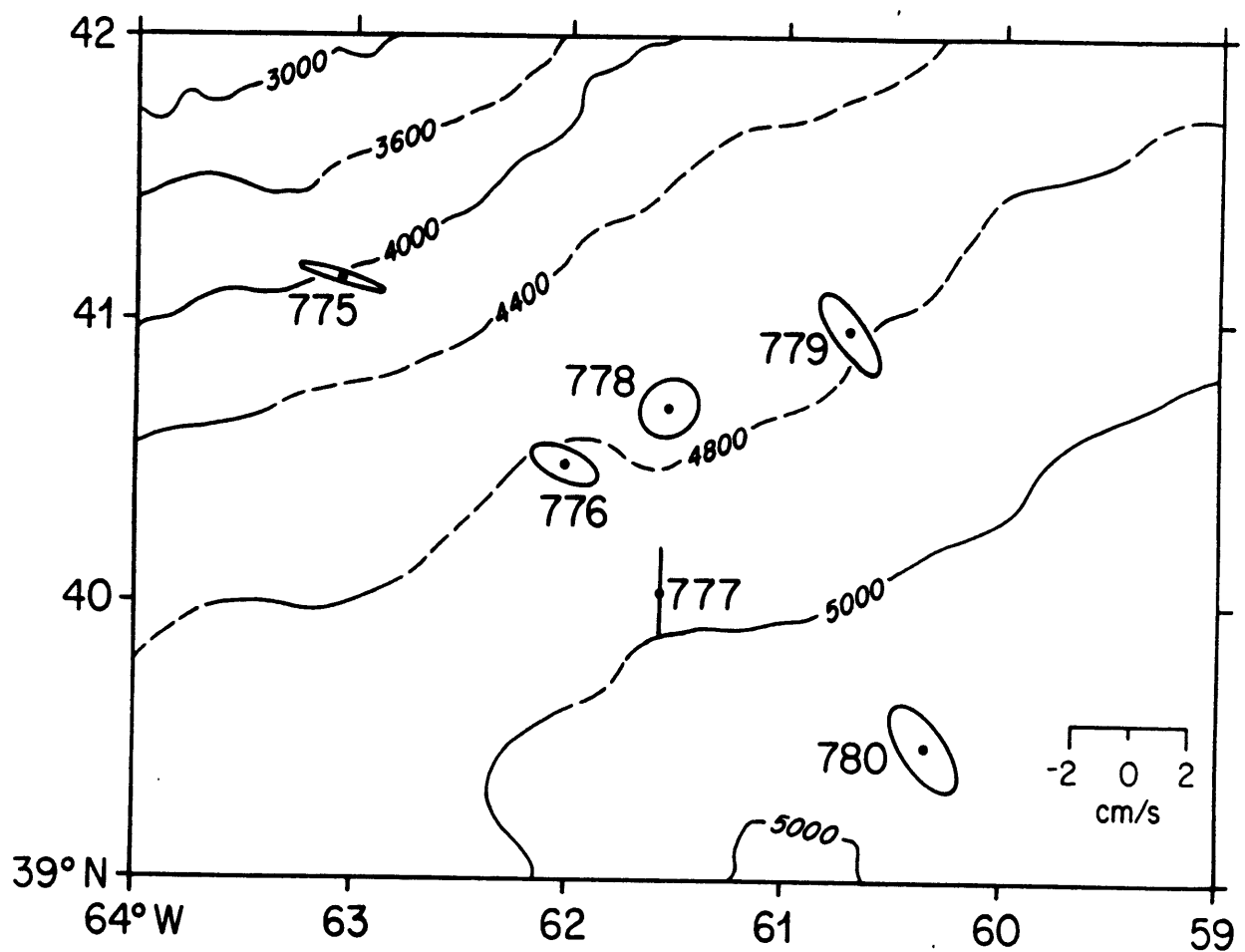


Figure 2.14: Variance ellipse representation of deep horizontal modes in the 17 day band.

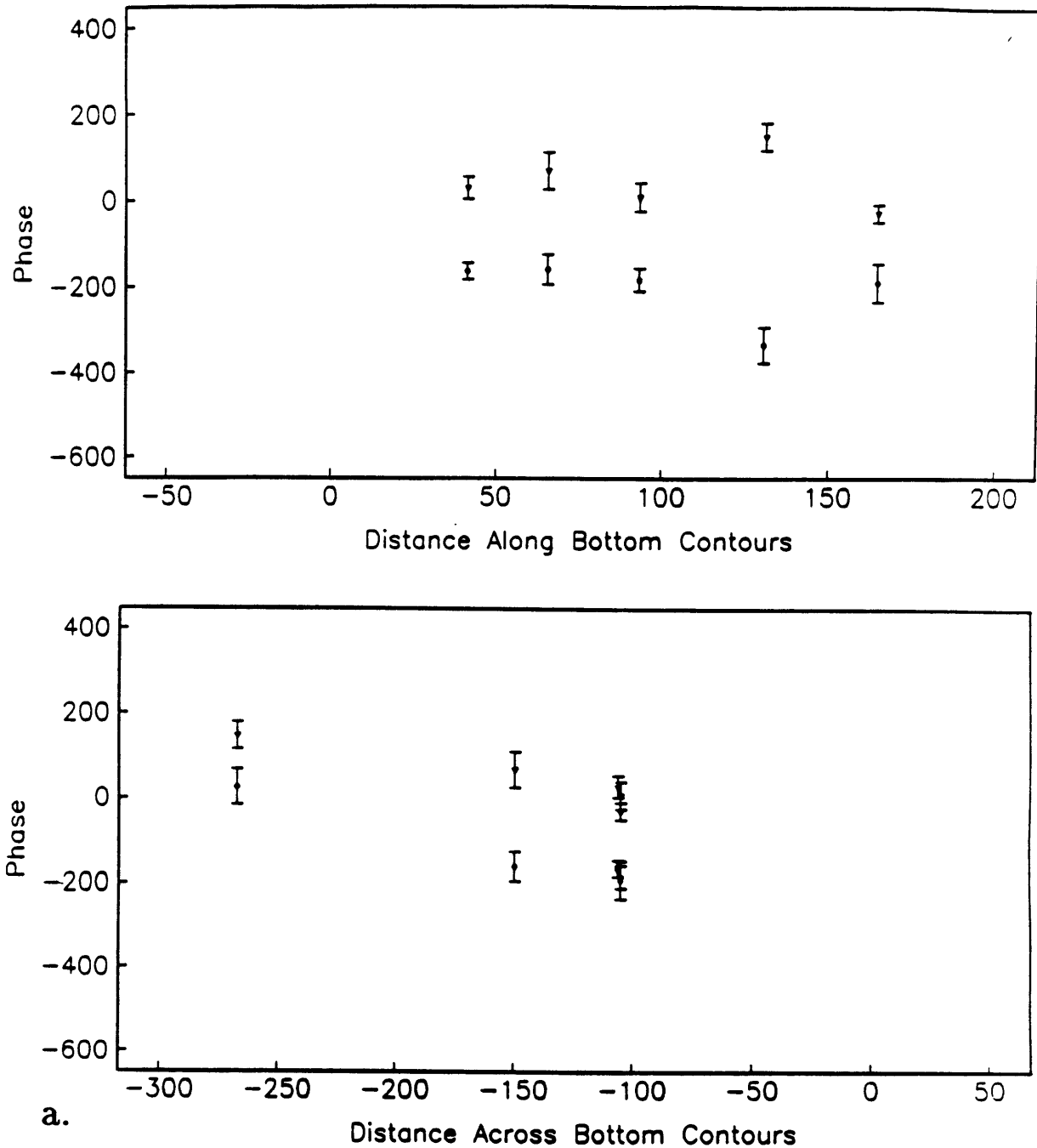
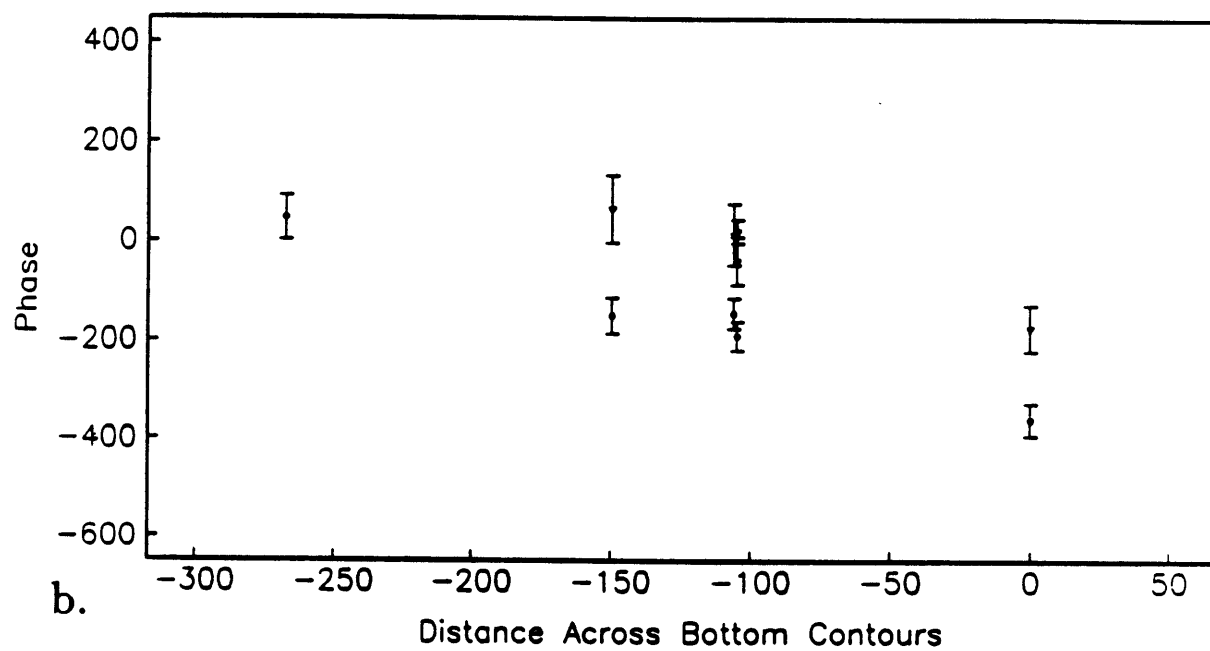
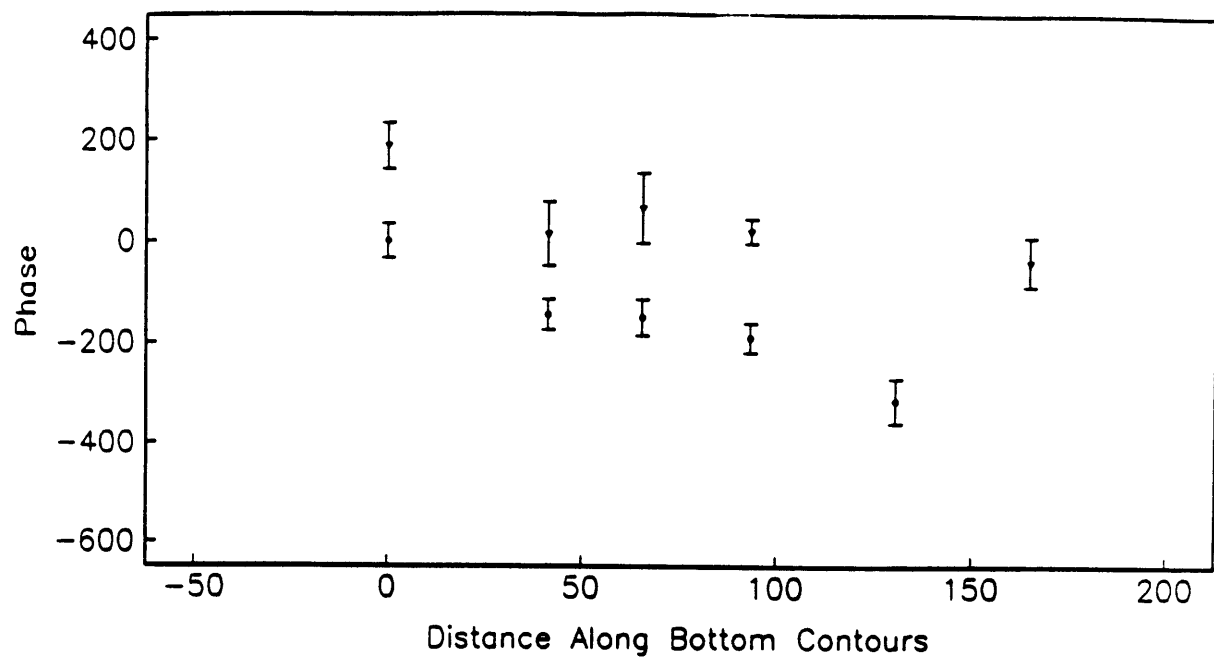
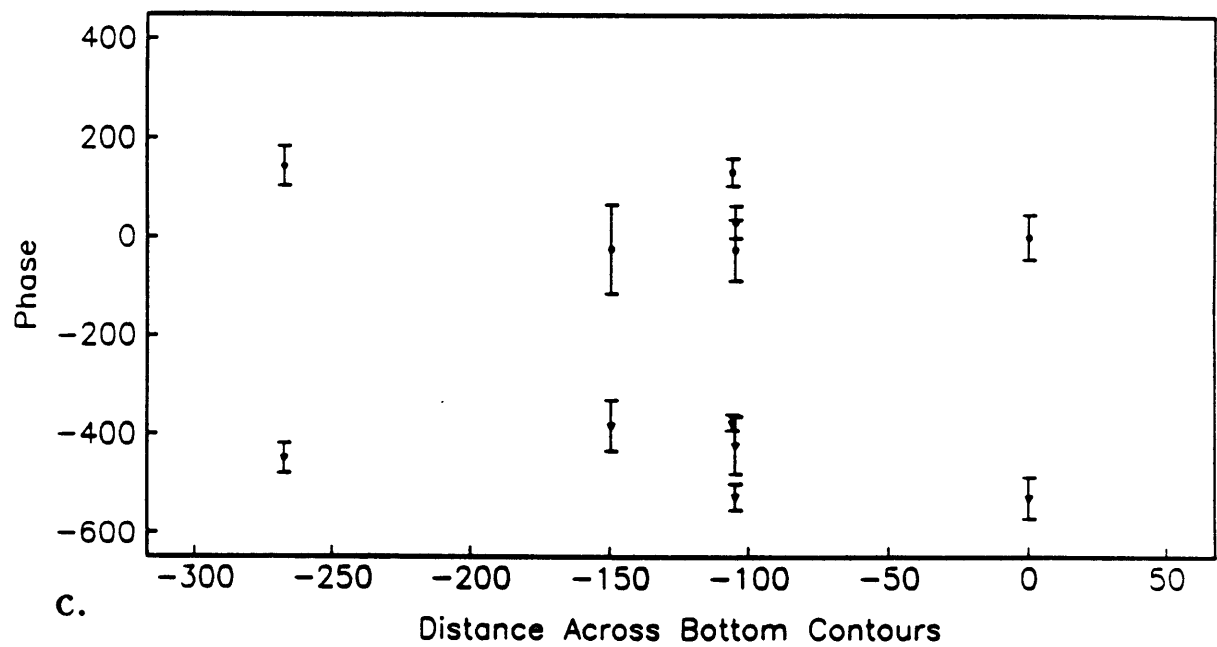
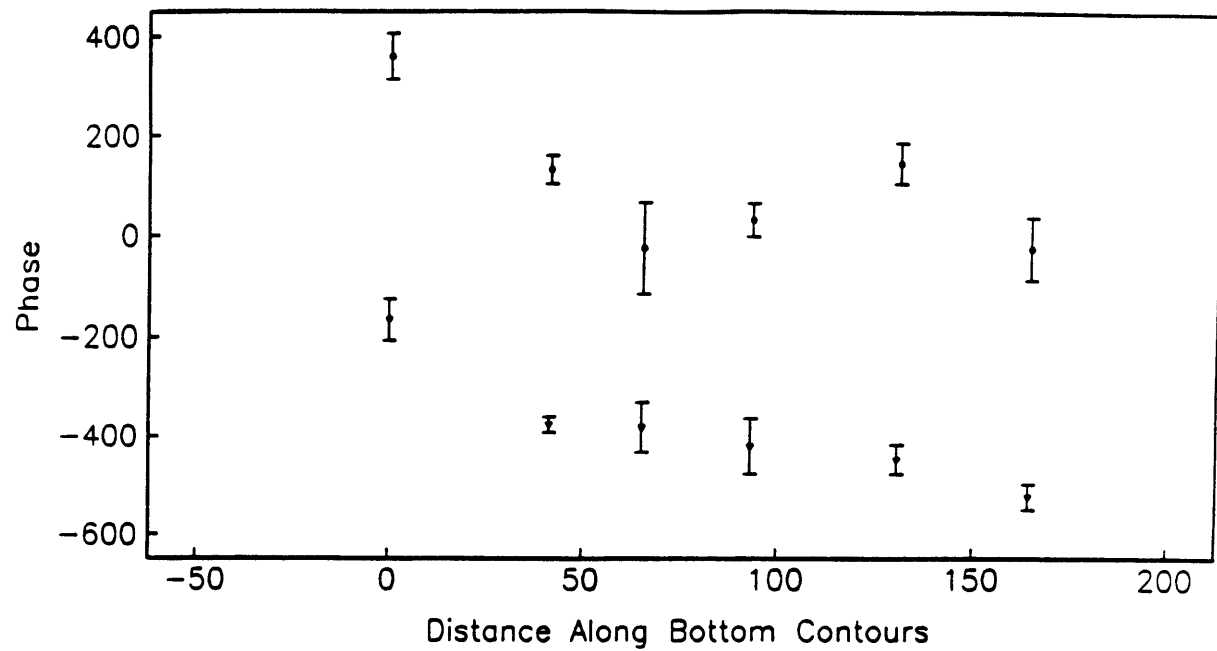


Figure 2.15: Phase propagation along and across isobaths in a. the 120 day band, b. the 30 day band, and c. the 17 day band. The circles are phase values associated with 'u' and the triangles are those associated with 'v' where the direction of the components is dependent upon the coordinate system used for that band (see text).





Inst.	120 days		30 days		17 days	
	coh u	coh v	coh u	coh v	coh u	coh v
7753	46	29	76	66	66	69
7765	89	83	78	58	80	92
7771	74	69	73	56	50	63
7781	81	77	79	84	76	60
7791	67	88	42	65	58	82
7806	69	77	67	53	70	78

Table 2.3: Coherence amplitudes calculated from the listed data series and the modal series from the horizontal analysis of 4000 meter records. The direction of u and v is different for each band depending upon the coordinate system used in the analysis (section 2.2.1). An amplitude of 62 is significant at the 95 percent confidence level.

be expected. In addition, f will change in the along isobath direction so this relationship will not be strictly linear, but these variations are smaller. For these reasons and because there are so few moorings, it is difficult to make good estimates of wavenumbers. However, it is clear that phase propagation is to the southwest in all three bands. This suggests that the observed motions might be topographic Rossby waves with an associated shoreward flux of energy. In the next section the general characteristics of these waves will be compared to the theory.

2.3 Topographic Rossby waves: a review

In regions where the effects of topography begin to compete with the β effect, as in the ABCE region, potential vorticity conserving motions must also respond to these changes in the depth of the fluid. Quasigeostrophic topographic Rossby waves in a stratified ocean must obey the following equation for the streamfunction:

$$\frac{d}{dt} \left[\nabla^2 \psi + \frac{\partial}{\partial z} \left(\frac{f^2 \psi_z}{N^2} \right) + \beta y \right] = 0$$

where

$$fu \approx -\psi_y \text{ and } fv \approx \psi_x$$

subject to the boundary conditions

$$\psi_x = 0 \text{ at } z = 0,$$

$$\frac{d}{dt}\psi_x = N^2 u \cdot \nabla h \text{ on } z = -H.$$

Assuming that changes are gradual in horizontal directions, this equation can be solved locally and variations can be approximated by changing the parameters of the problem. For the purpose of examining the effects that changes in bottom slope and mean flow have on the resultant wavenumbers in the various frequency bands, the assumption was made that variations occur only in the meridional direction.

Dispersion relations of the linearized equation were then found numerically, using reasonable values of relevant parameters from the locations of moorings 775, 776, and 780 and using profiles of buoyancy frequency calculated from CTD measurements made during the experiment. Figure 2.16 shows a typical buoyancy frequency profile for the region. A relevant parameter is β_t/β , which measures the effect of topography relative to β . The topographic beta term, β_t , is given by fh_y/H . The best choice for h_y is an average over a wavelength, and very rough estimates from the phase diagrams indicate that these are on the order of a few hundred kilometers. Taking this into consideration, approximate values calculated for β_t/β are 11, 3.8, and 1 for 775, 776, and 780 respectively. Mean flow values used were -5 , -3 , and 4 cm s^{-1} . Mean flow is assumed to be independent of depth.

In figure 2.17, which shows comparisons of the dispersion relations for the nearly barotropic mode at the three sites for each period, mean flow was not included in the model. Primarily, the effects of changes in bottom slope cause the changes observed. Vertical structures for a zonal wavenumber of -0.01 km^{-1} are next to each dispersion curve. By comparing the three figures the effects of variable frequency at a given site can also be observed.

Since the assumption has been made that changes occur in the meridional direction only, a given wave should have the same zonal wavenumber, k , at each of the three sites. For a given k , the meridional wavenumber, l ,

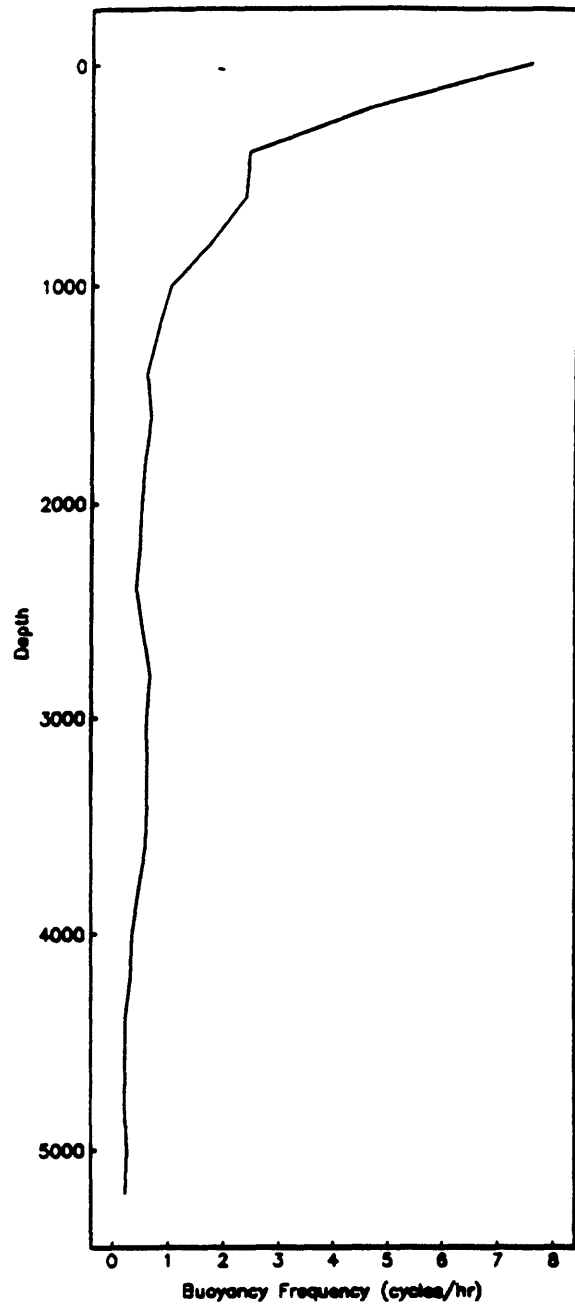


Figure 2.16: Buoyancy frequency vs. depth taken from a CTD station made in June, 1983 and located at 60.5W, 39.5N. The values plotted are those used in determining a solution of the potential vorticity equation at mooring 780. There is a depth averaged value for every 200 meters.

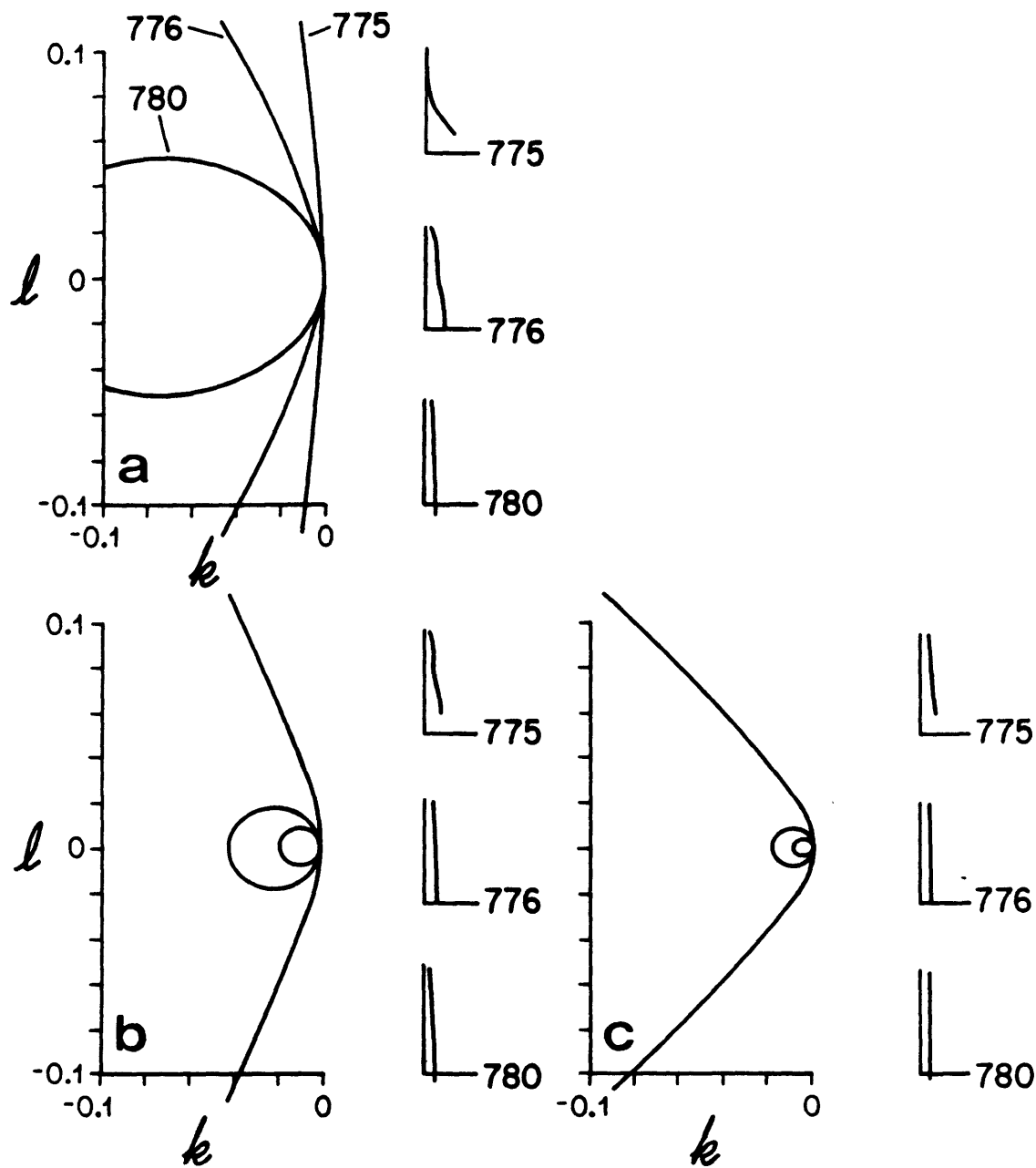


Figure 2.17: Dispersion relations for the near barotropic mode calculated numerically using estimated parameters for the three moorings in a. the 120 day band, b. the 30 day band, and c. the 17 day band. To the right of the dispersion curves the vertical structure is shown for each location. A zonal wavenumber of -0.01 km^{-1} was used in the calculation. Mooring labels for the curves are as in figure a. (Axes for vertical structure curves were created for parameters at mooring 776.)

increases considerably as the slope increases, and as motions are perpendicular to the wavenumber vector they should become more along isobaths. The three figures show how this alignment is a function of frequency. As the restoring force is larger for cross isobath motions the associated frequency is higher, therefore the meridional wavenumber at a given location is smaller for high frequencies as is shown in the dispersion diagrams.

Figure 2.18 shows the model after mean flow has been included. Because in the region of interest the slope does not vary strictly in the meridional direction, the inclusion of the mean flow in the problem complicates the dynamics, as variations in the x direction in topography or in f (if along isobath coordinates are used) imply that modifications in the mean flow must also occur for the mean flow itself to satisfy the quasigeostrophic potential vorticity equation. With variations in the flow field the model would be very difficult to solve. However, β_t quickly dominates over β so that in along isobath coordinates it can be assumed that the along isobath component of f , and therefore the mean flow, remains constant and the qualitative changes the latter might produce can be examined. Inclusion of mean flow only affects waves with relatively high zonal wavenumbers, as these waves have phase speeds which are comparable to the mean flow speeds. The effect of a westward mean flow is to intensify the increase in meridional wavenumber. For an eastward mean flow, the effect is the opposite. Therefore, as the mean flows become increasingly more westward to the north in the ABCE region we should expect slightly more enhancement of l than would be expected in an ocean at rest.

Returning to the ellipse diagrams, these characteristics of topographic Rossby waves are clearly illustrated. The motions in the band centered at 120 days are alligned along bathymetric contours, whereas motions in the 17 day band are much more across contours. Motions in the 120 day band at mooring 775 are not coherent with those to the south. Because the meridional wavenumber increases most rapidly with increasing slope parameter for low frequency waves, the ambient field at 775 is probably no longer able to support those waves observed over smaller slopes to the south. Referring to the dispersion diagram this would be expected for all waves in the 120 day band except those with very large zonal scales. There is energy in the 120 day band at mooring 775, but it shows up in the second empirical mode implying that it may have a different energy source.

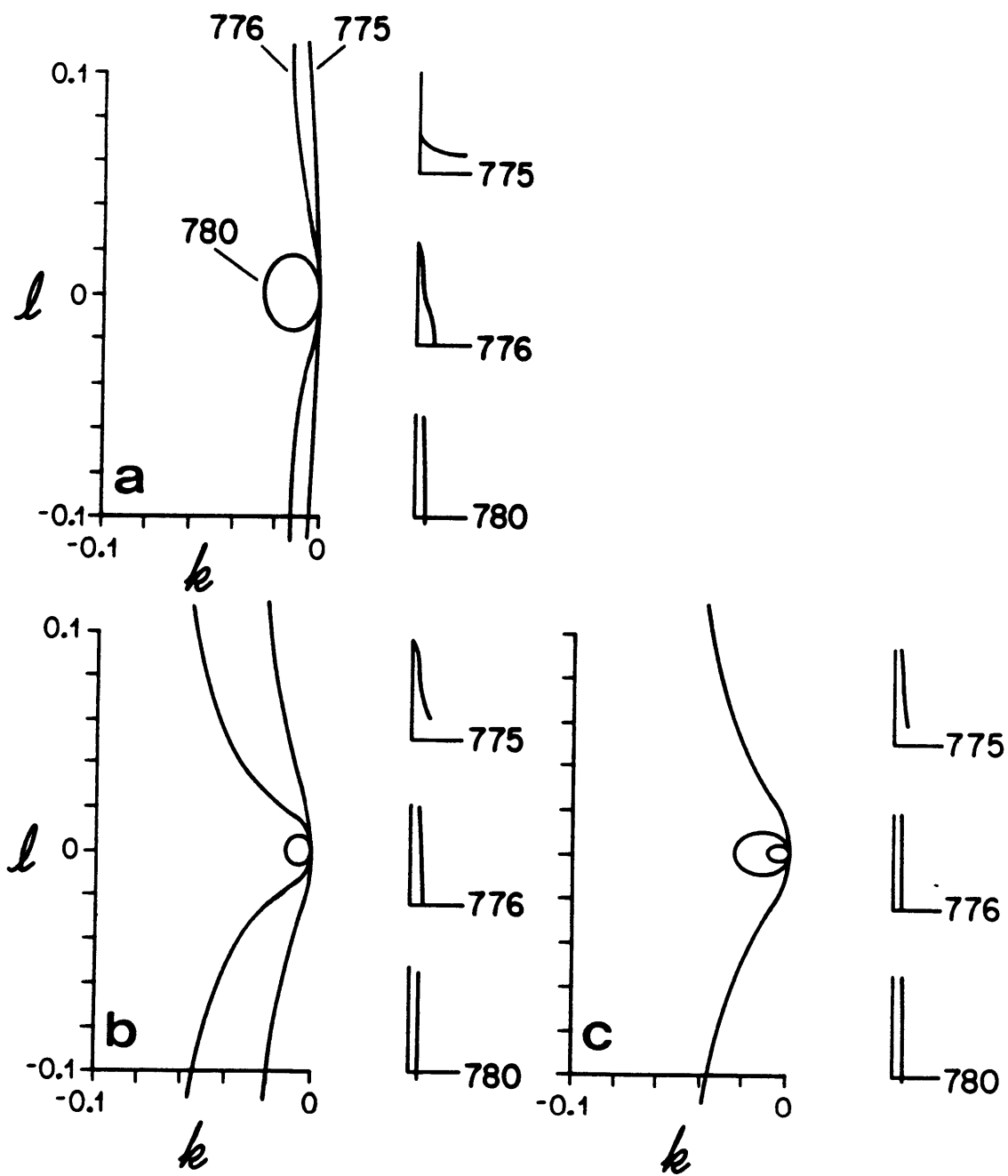


Figure 2.18: As in figure 2.17 with mean flow included in the model.

The vertical structure will also change as a function of position and mean flow. If the buoyancy frequency is assumed constant then the vertical structure is proportional to $\cosh(K_h N/f)$, (Rhines, 1970), and because the meridional wavenumber increases with increasing slope, decreasing mean flow, and decreasing frequency, the trapping scale should decrease with these changes. This can be seen in the vertical structure plots next to the dispersion curves. It can also be seen in the data in figures 2.8–2.6. Motions are clearly more bottom trapped at mooring 775 than they are to the south. The largest bottom slopes and the most negative mean flows are observed at this mooring site.

Although the amplitudes of these waves at 4000 meters are nearly uniform over the array this trapping indicates that the vertically integrated kinetic energy is decaying to the north. For example, the integrated energy in the 17 day band was estimated at each mooring site. At most locations it was assumed that the motions were depth independent and the amplitude of the major axis component of the velocity associated with the deep horizontal mode was assumed to be the amplitude over the full water column. At mooring 775 a wavenumber was estimated and the vertical structure was calculated from topographic wave theory. Again, the 4000 meter amplitude was taken from the horizontal mode calculated from the data, and the energy was estimated by integrating over the water column. Because the wavenumbers are difficult to determine, they were adjusted until the vertical decay from the model was similar to that observed in the vertical modes calculated from the data. Values for k and l of -0.02 km^{-1} and -0.046 km^{-1} were chosen. Very rough estimates of $\int A^2 dz$, where A is the amplitude of the disturbance, give values of $6.7 \times 10^5 \text{ cm}^3/\text{s}^2$ and $3.3 \times 10^5 \text{ cm}^3/\text{s}^2$ at moorings 776 and 775 respectively, showing significant decay.

The most interesting result of the horizontal analysis is that these motions are coherent over such a large horizontal scale. Also, the flux of energy is shoreward. It is at least plausible that these motions were forced in the region of the Gulf Stream. In the next chapter this relationship will be examined in more detail.

Chapter 3

Gulf Stream Variability

In the preceding chapter it was demonstrated that motions on the Continental Rise are coherent with mooring 780 in the Gulf Stream in some frequency bands. In this chapter the hypothesis that the Stream is a source for this low frequency variability is explored. Year long current meter records from the SME moorings in conjunction with records from mooring 780 from the ABCE array permitted an analysis of the horizontal and vertical structures of the Gulf Stream. Table 3.1 shows the information about the moorings in the Synoptic Mapping Experiment.

3.1 Time domain

Stick plots of the records at three moorings—558, 557, and 560—are shown in figures 3.1, 3.2, and 3.3. Again, the presence of the Stream and related features is apparent from the strong amplitudes and surface intensification of the current, and high temperatures at the uppermost level at each mooring. A noteworthy feature clearly illustrated in the stick plots is the vertical coherence, especially in the latter parts of the records. At all locations in the array during the times when the Stream is over the mooring it extends to the level of the deepest instruments. This was noted in section 2.1 in the discussion of mooring 780, and demonstrated again in the frequency domain analysis of the vertical structure at that mooring site (section 2.2.1), but the SME data shows that this is generally true in this region.

The extension of eastward flow in the jet to the bottom eliminates the possibility that far field waves are forced by the radiation instability mechanism described in chapter 1. Talley (1982) found that all radiating modes

Inst.	Start Date	# Days	Depth (m)	Water Depth	Lat.	Long.
5571	5-07-83	283	445	5167	39.50	-58.97
5572	5-07-83	358	850	5167	39.50	-58.97
5573	5-07-83	358	1355	5167	39.50	-58.97
5574	5-07-83	277	3959	5167	39.50	-58.97
5581	5-08-83	357	467	5140	39.98	-59.00
5582	9-29-83	213	872	5140	39.98	-59.00
5583	5-08-83	357	1377	5140	39.98	-59.00
5584	5-08-83	357	3981	5140	39.98	-59.00
5592	5-08-83	358	878	5196	39.49	-58.33
5593	5-08-83	358	1384	5196	39.49	-58.33
5594	5-08-83	358	3988	5196	39.49	-58.33
5601	5-11-83	356	495	5169	39.02	-59.03
5602	5-11-83	356	900	5169	39.02	-59.03
5604	5-11-83	356	4010	5169	39.02	-59.03
5611	5-11-83	356	479	5152	39.54	-59.67
5612	5-11-83	356	884	5152	39.54	-59.67
5614	5-11-83	356	3993	5152	39.54	-59.67

Table 3.1: The Synoptic Mapping Experiment array.

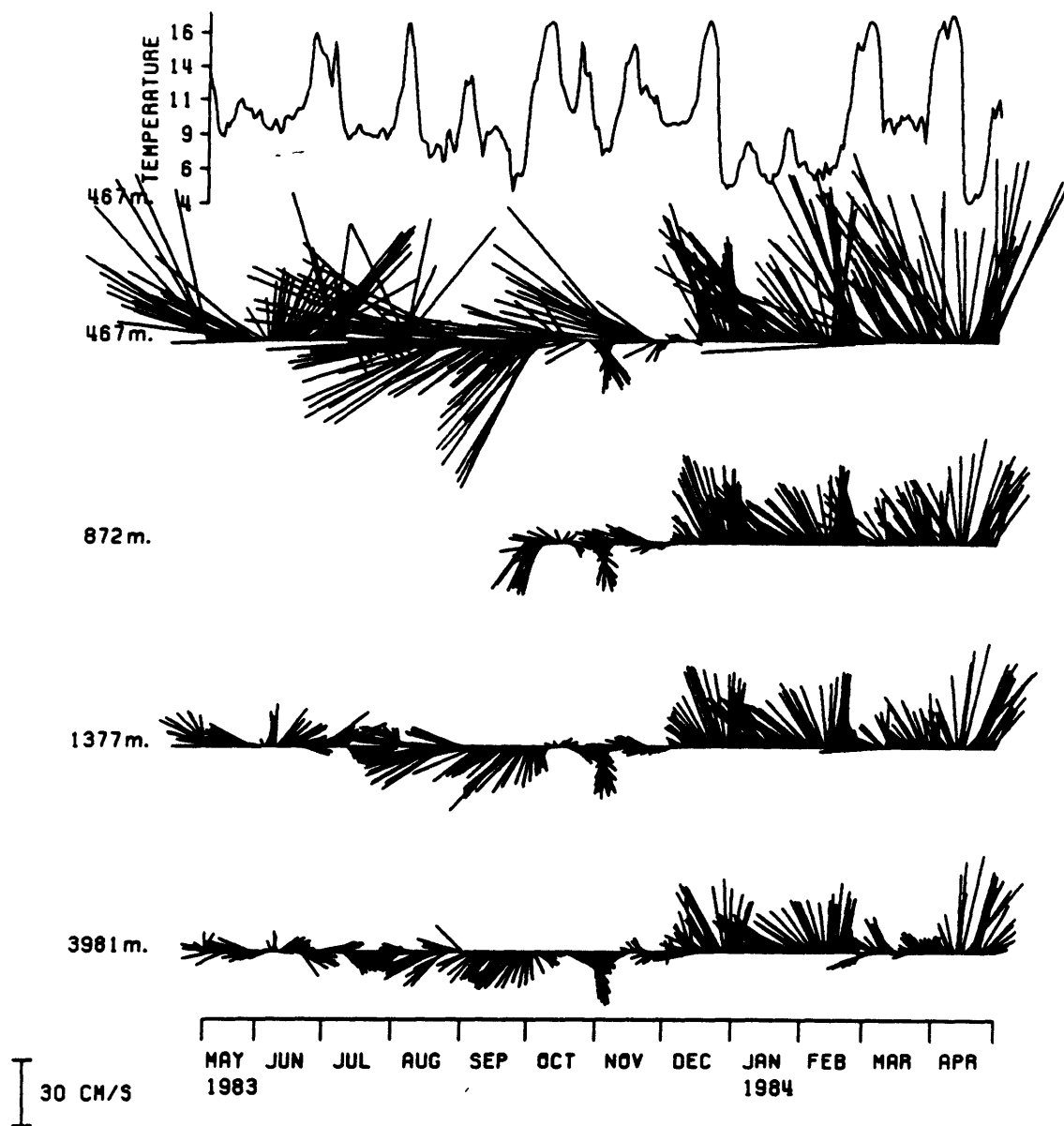


Figure 3.1: Temperature at 445 meters and stick plots at mooring 558. East is up.

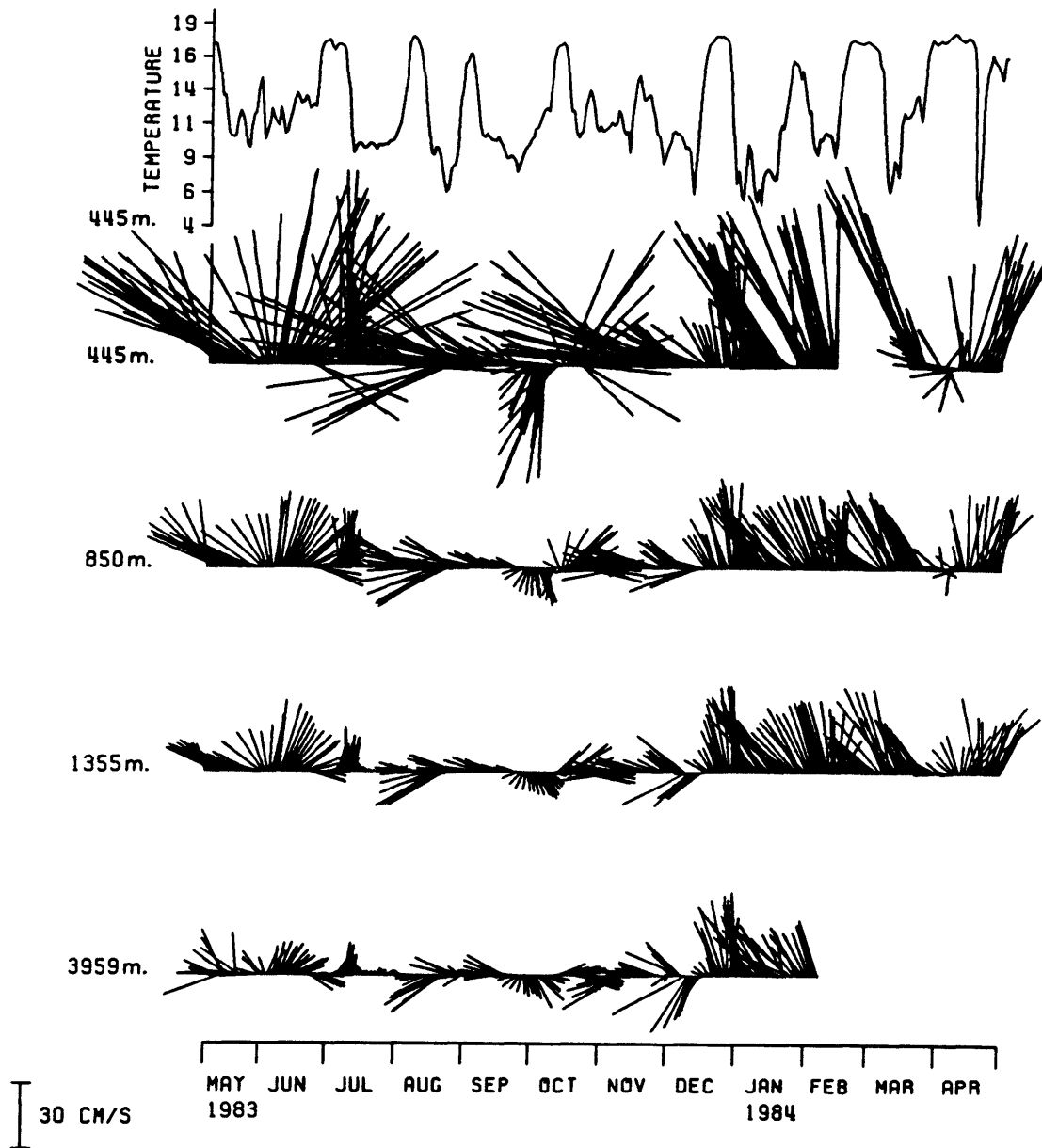


Figure 3.2: Temperature at 445 meters and stick plots at mooring 557.

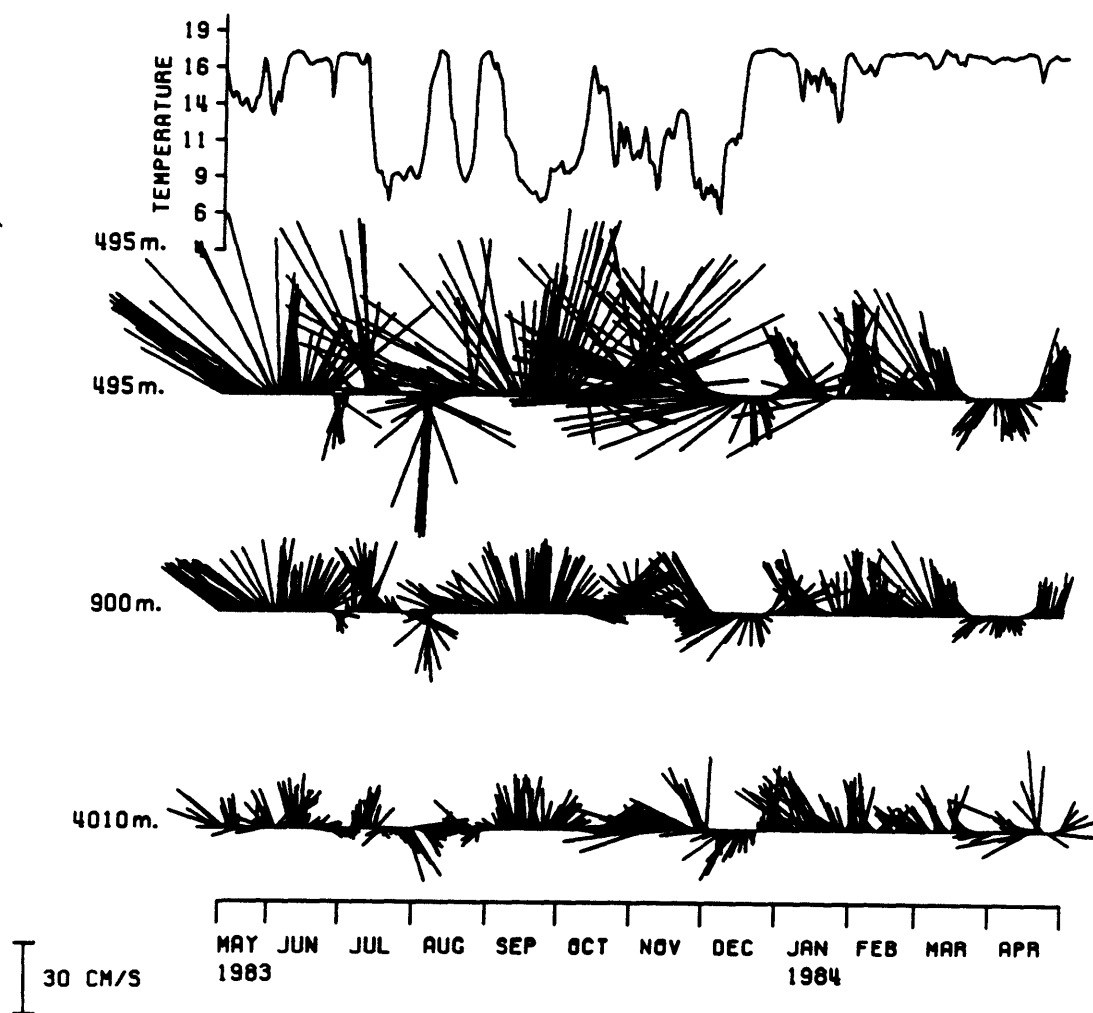


Figure 3.3: Temperature at 495 meters and stick plots at mooring 560.

have phase speeds within the range of the flow speeds and therefore the waves generated by this process in the vicinity of the ABCE and SME arrays must have positive zonal phase speeds. The phase speeds of the observed waves are negative as they must be in a westward flow field. Therefore the far field is incapable of supporting waves excited by the instability process. It is unlikely that topography will affect this conclusion since positive bottom slope tends to enhance the β effect and would be expected to inhibit destabilization. On the other hand, Talley showed that in the presence of positive vertical shear in the far field those waves which are destabilized and trapped became radiating at high β . However, in her model with positive vertical shear in the far field, only positive far field flow speeds were examined. As the far field flow speeds were themselves in the range of the jet flow speeds radiation was possible because Rossby wave speeds could take on positive values. This is not the case in the ABCE region because while far field vertical shear is positive, the flow speeds are not.

Returning again to the stick diagrams, two separate flow regimes can be observed in both space and time. Strong eastward motions occur at all Gulf Stream moorings, excluding mooring 560, beginning in the middle of the month of December and lasting throughout the remainder of the records. The Stream is clearly present during this time with little change in direction. The preceding months show more variability in direction although the upper level flows usually are comparable in strength to those in the second part of the records. The surface intensified but highly variable flow at the two more northern moorings appears to be the signature of strong meanders and Gulf Stream rings. Rings and meanders propagating over the mooring site appear in the records as a rotary progression of vectors over time. Strong westward flows at 500 meters are not unusual in the case of a ring, and are often observed during the early parts of the records.

Flows at the southernmost mooring in the SME array, mooring 560, are strong, surface intensified, and primarily directed to the east from the start of the experiment until approximately November. During this time Stream related features are present over all mooring sites in the array. Apparently the Stream is displaced to the south as warm core rings are shed to the north over the remaining moorings, or strong meanders have allowed passage of the Stream over all the moorings in the array. After November the currents at 560 are reduced in amplitude at the shallowest instruments and are much

more depth independent, resembling the nearly barotropic motions to the north of the Stream, for example at mooring 776. The temperature records are much less variable during this part of the record with high values as would be expected in the Sargasso Sea.

The sea surface temperature maps released by the National Weather Service support these general observations. There is much more warm core ring activity over the northern moorings before December, 1983, with the Stream itself often in a more southern position. After this time the Gulf Stream follows a fairly smooth course to the east over the more northern moorings for the duration of the experiments. During this time there are few Gulf Stream rings near any of the moorings. Figures 3.4 and 3.5 show examples of typical maps during the two time periods.

Two regimes have been described and will be referred to later in the text. To summarize, all records change character in November or December of 1983. The northern moorings change from strong meanders and rings which are manifested in highly variable direction of surface intensified flows, to a more unidirectional eastward flowing Gulf Stream. The southern mooring, 560, changes from a surface intensified flow which is probably a southward excursion of the Stream, to a nearly barotropic and less intense flow which is no longer in the main body of the Stream.

3.2 Frequency domain analysis of the SME data

Empirical orthogonal functions were used to examine the Gulf Stream time and space scales. The records from the SME array were shorter than those from the ABCE array and to get accuracy comparable to that obtained with the ABCE data, piecelengths used in calculating Fourier transforms were reduced. This results in larger bandwidths making direct comparisons to Rise motions sometimes difficult.

Because there is so much low frequency energy in the vicinity of the Stream, and because the bands are rather broad, interpretations of the modes are often difficult as it is possible that more than one process is represented by the mode. Most often the modal velocity ellipses are more circular than elliptical which can be an indication of this complexity. For example, suppose two Rossby waves are present, one propagating more nearly westward, the other having a larger meridional wavenumber compo-

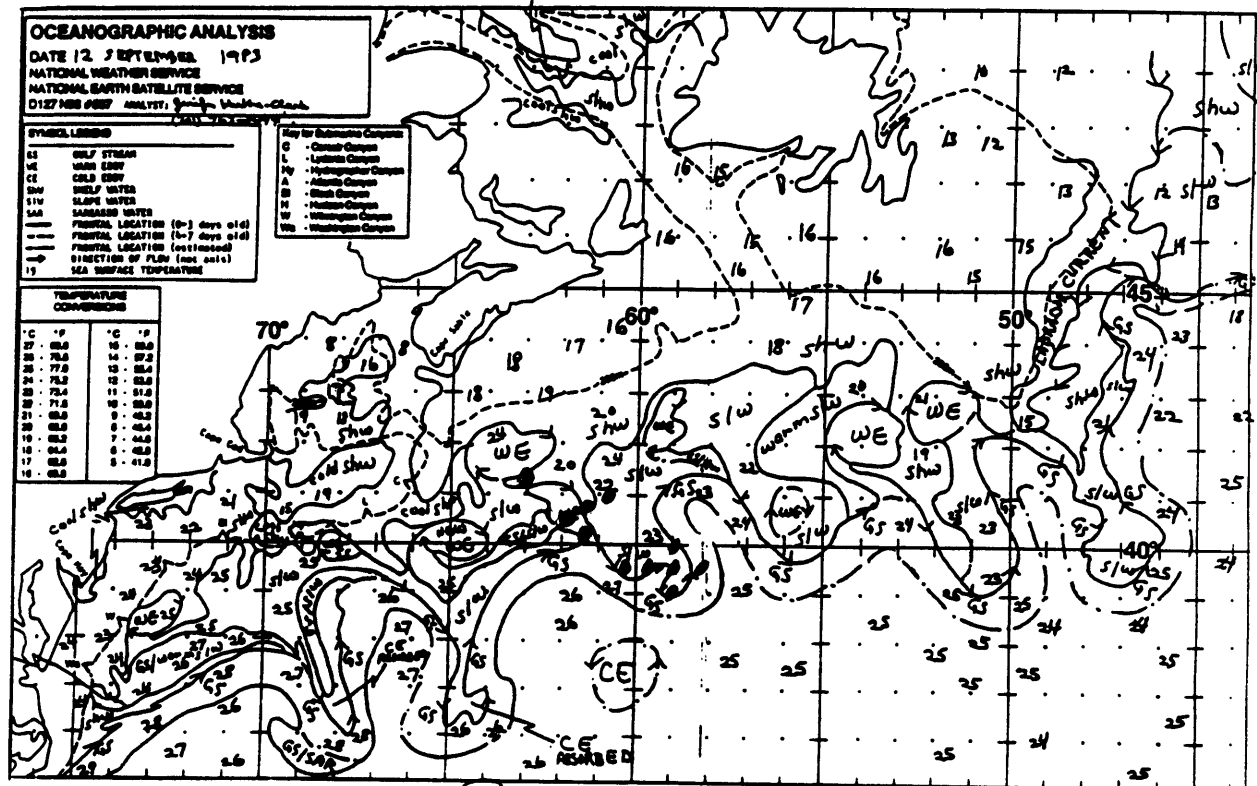


Figure 3.4: Plot of sea surface temperature and inferred flow field on September 12, 1983.

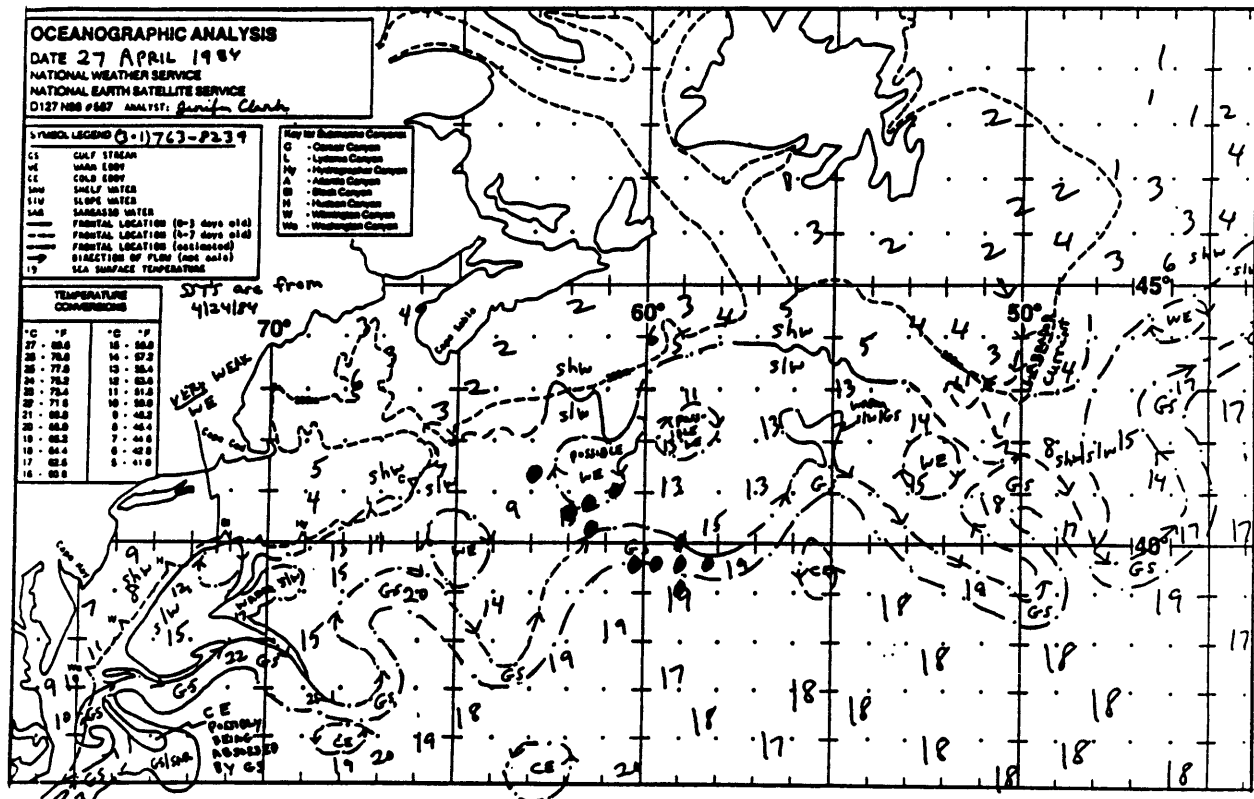


Figure 3.5: Plot of sea surface temperature and inferred flow field on April 27, 1984.

nent. The velocity perturbations of the wave will be directed more meridionally and zonally, respectively. As the velocity components are associated with two separate waves, they will not be in or out of phase. In addition, it is unlikely that the phase propagation associated with the two components will be the same. The passage of Gulf Stream rings over the mooring sites will also complicate the modes. Coherence between velocity components is not guaranteed because the time scales of associated fluctuations are likely to be different. Spatial coherence between records taken from different sites over which a ring passes is also unlikely. Time scales of fluctuations are dependent upon the cross-section of the ring sampled by the instruments and this will vary between moorings. Because of these complications, the emphasis where interpretation is difficult is more on time scales and direction of phase propagation rather than on the identification of specific types of disturbances.

In all the analyses that follow, there is a strong mode in the 30 day band. In the bands which include the remaining time scales concentrated upon in the ABCE analyses, the variance is more evenly split between the first two modes with no apparent reason on physical grounds for the split. Therefore the discussion will focus on the 30 day structure and an attempt will be made to compare it to the structure on the Rise. Clearly, this will not result in an explanation of the wave field on the Rise as motions there exist in all low frequency bands, but hopefully the discussion will be suggestive of possible Gulf Stream forcing mechanisms. In the following sections the general features of the vertical and deep horizontal structures in the 30 day band are described.

3.2.1 Vertical structure

The vertical structures of the modes in the 30 day band at three of the moorings are shown in figure 3.6. Note that mooring 559 does not have a 500 meter record which accounts for the more depth independent appearance of the modal amplitudes. The remaining modes are similar to those at mooring 780 in the ABCE array (figure 2.7). Motions are strongest at the 500 meter instruments and are nearly constant below that level. Phase differences between velocity components are closer to 90 degrees than 0 or 180 degrees making the ellipses less elongated. However, at the southernmost

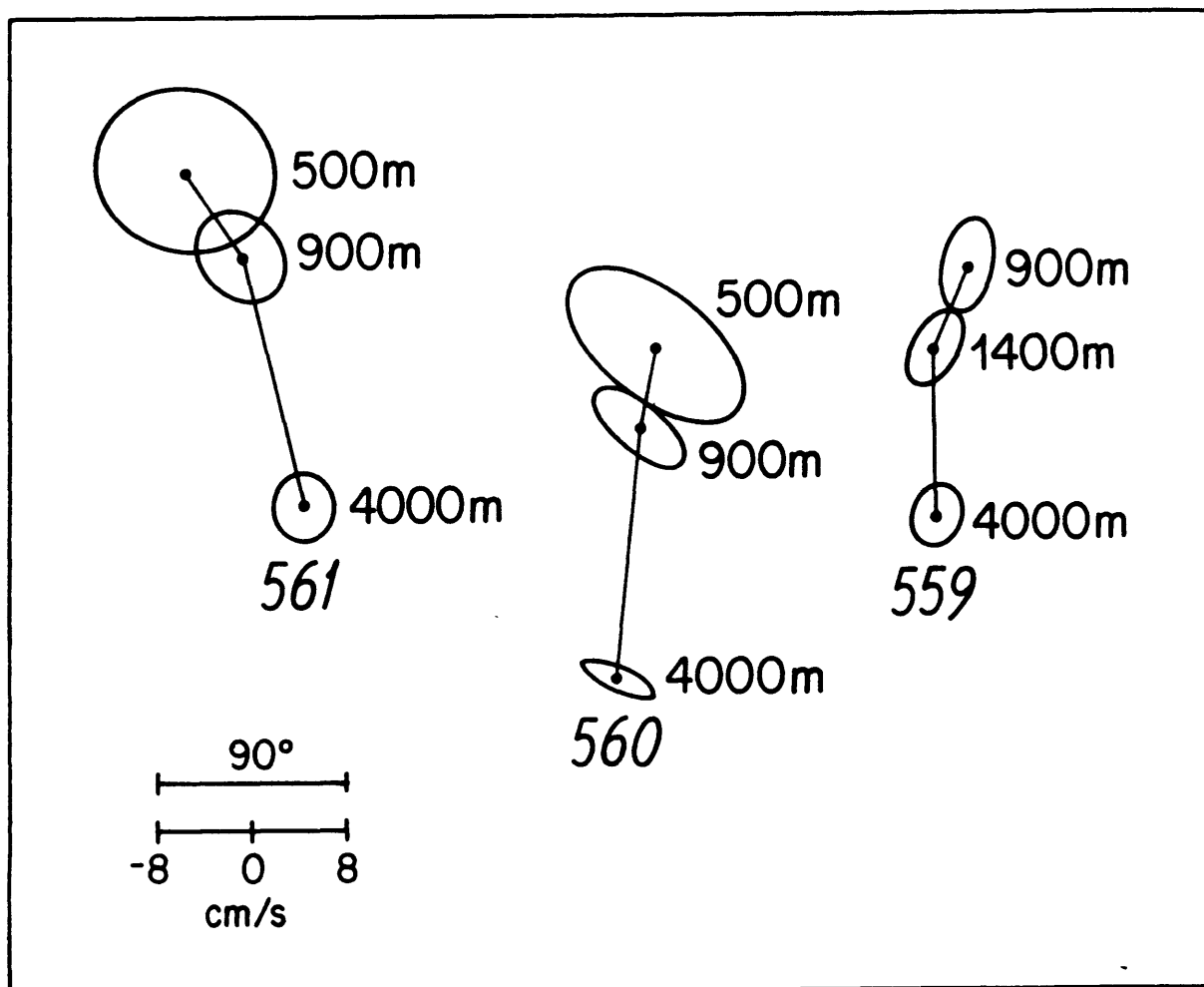


Figure 3.6: Vertical structures of the first modes in the 30 day band at moorings 561, 560, and 559 from the SME array.

mooring, 560, motions are slightly more transverse especially at 4000 meters. This more wavelike feature may in part result from the contribution from the latter part of the record during which the Stream has migrated north. At mooring 561 the largest vertical phase shifts of the major axis velocities are observed. This could be a signature of baroclinicity and might be related to ring activity.

3.2.2 Horizontal structure

To describe the deep horizontal structure of the Stream, records from the 4000 meter instruments from all moorings from the SME array and mooring 780 from the ABCE array were used to construct an empirical mode. Twelve months of data from most locations were used although the instrument at mooring 557 failed after 9 months. Fifty one percent of the variance in the 30 day band is explained by the first mode. The deep current ellipses (figure 3.7) are similar to those calculated in the vertical analyses. Coherence amplitudes are also listed in the figure. As in those modes the associated motions are more circular than transverse.

More interesting than the current ellipses are the plots of phase propagation (figure 3.8). Phase of the north component of velocity, v , decreases from west to east indicating westward phase propagation. In addition, a comparison to the phase plots of the ABCE horizontal analysis shows that the along bathymetry wavenumber of the Rise wave is quite similar to that associated with v in the Gulf Stream mode (figure 3.9). Because the zonal wavenumbers are comparable it is possible that there is a connection between the wave associated with the meridional component and the motions on the Rise. In fact, the 30 day modal ellipse at mooring 780 in the Rise analysis (figure 2.13) is directed primarily in the meridional direction. In contrast, the east component of the Stream modal velocity appears to have a very small positive associated zonal wavenumber. This eastward propagation can explain why this component at mooring 780 is not significantly coherent with wave motions on the Rise. If motions can be excited directly by wave motions in the vicinity of the Gulf Stream then the phase speeds of the waves must match those of free waves in the far field. Therefore they must be negative, and negative phase speeds are associated with only the meridional component of the velocity.

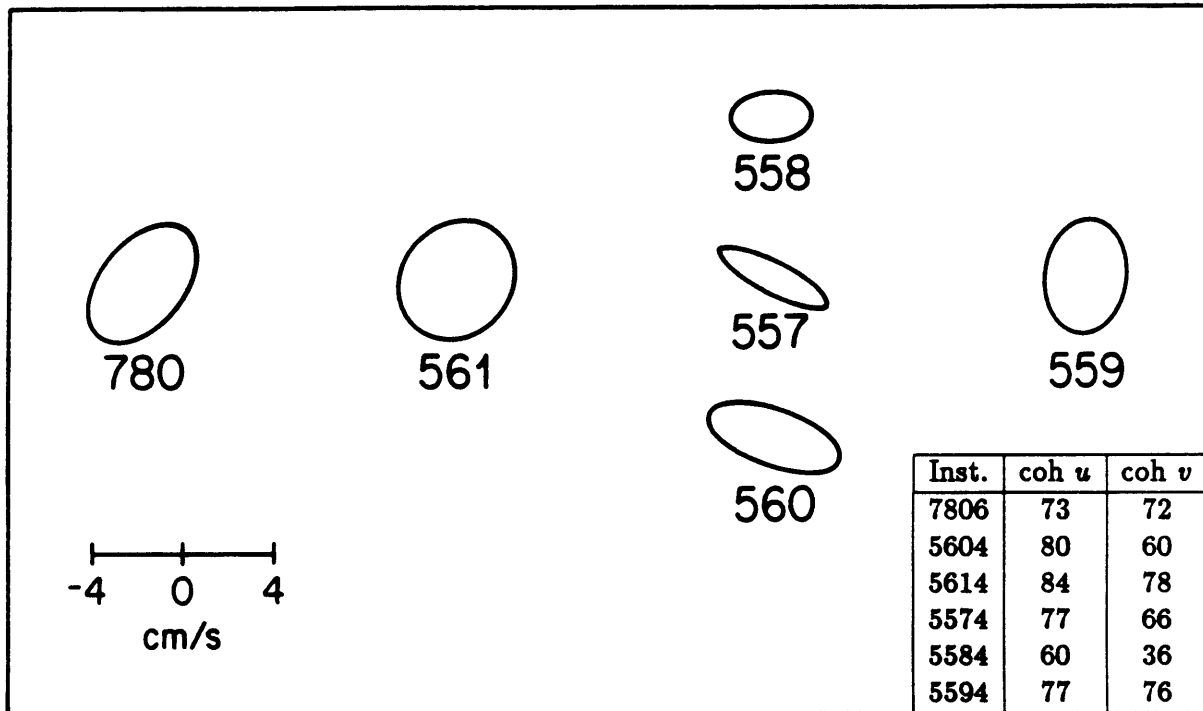


Figure 3.7: Current ellipse representation of the horizontal 30 day mode calculated from Gulf Stream records from 4000 meters. Coherence amplitudes between the data series and the modal series are listed in the table in the lower right corner.

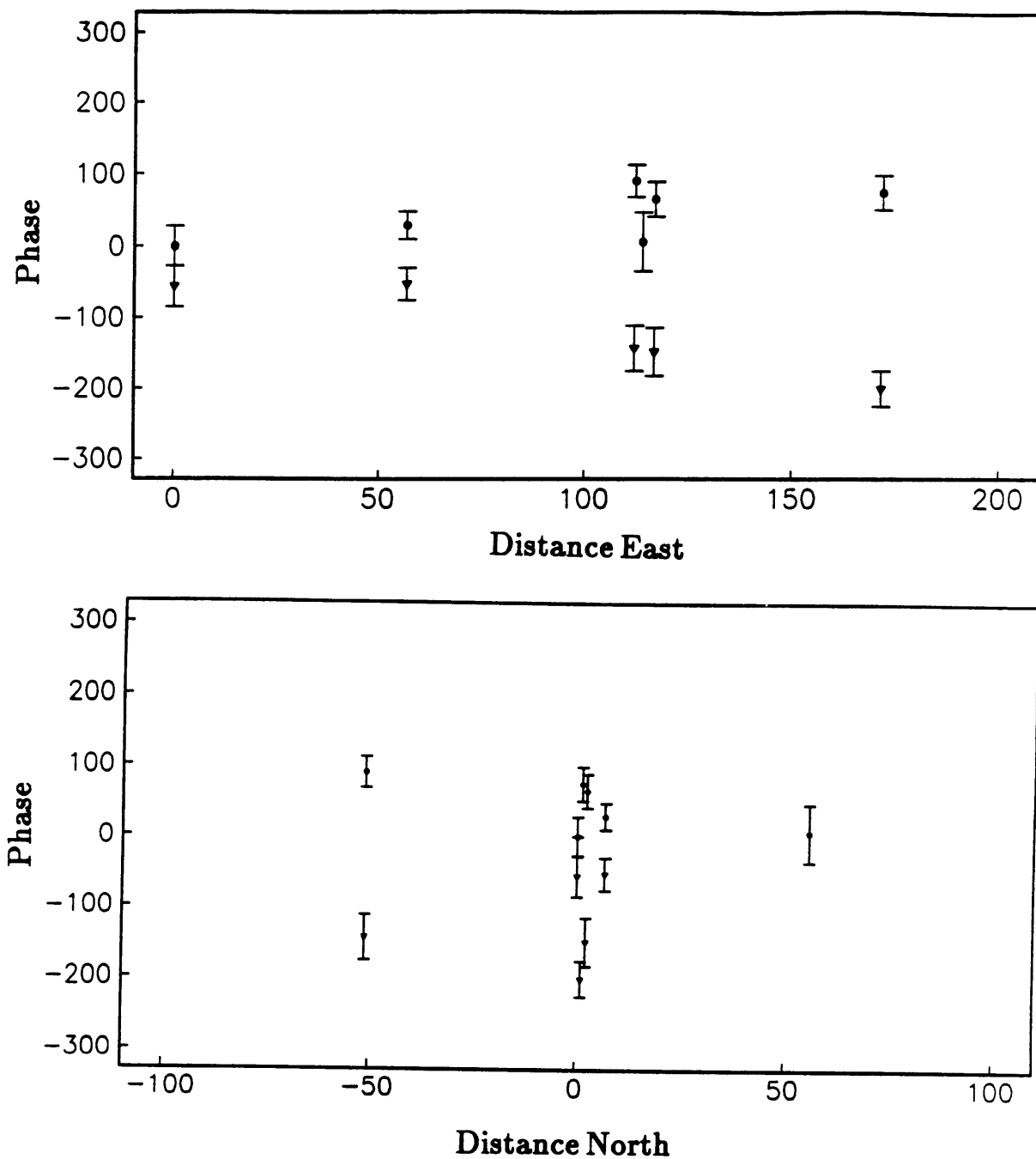
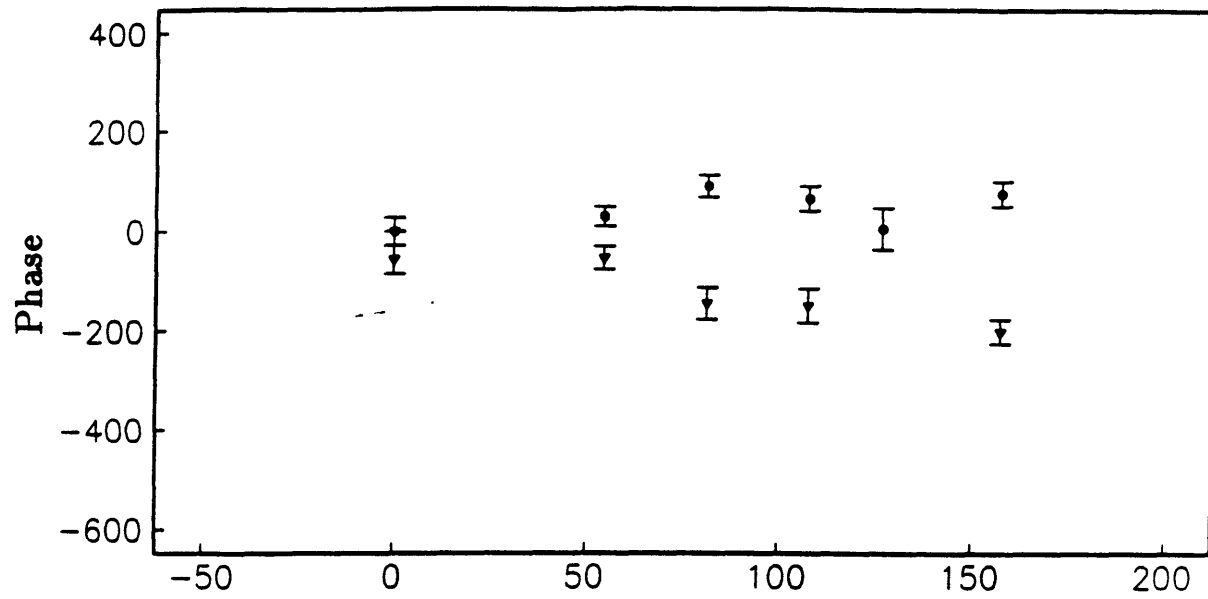
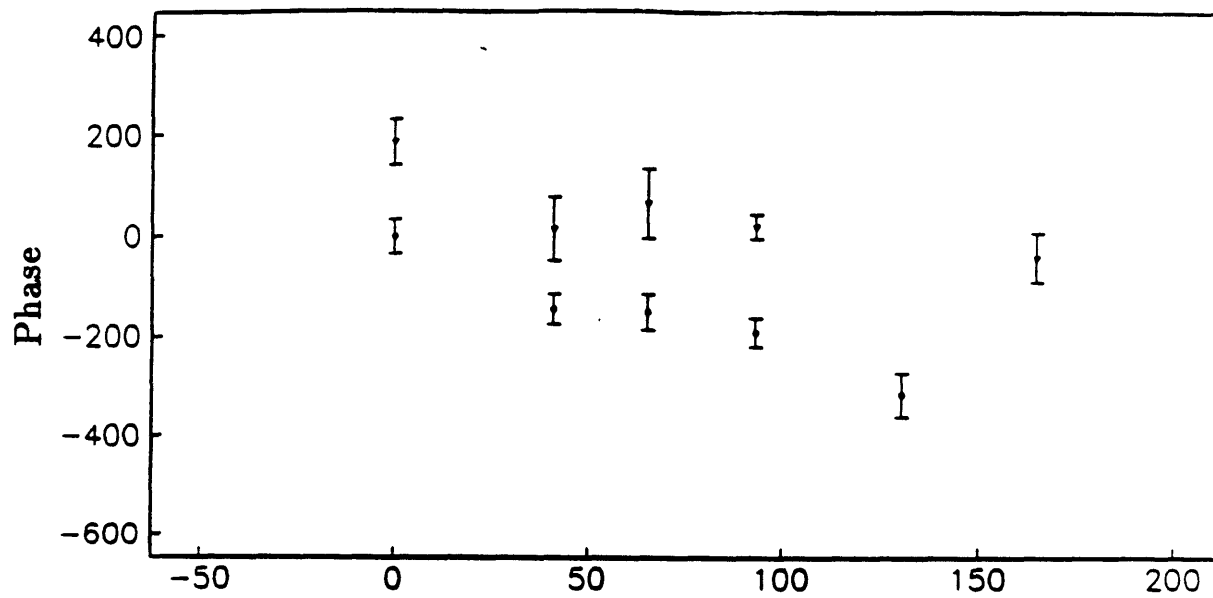


Figure 3.8: Phase in degrees plotted against distance east and north in kilometers for u (circles) and v (triangles) components from the first deep horizontal mode calculated from Gulf Stream records.



a.

Distance along bottom contours



b.

Distance along bottom contours

Figure 3.9: Phase plotted against distance along 24 degrees counterclockwise of east. a. Gulf Stream mode. b. Rise mode.

3.3 Gulf Stream forcing of Rise motions

In the frequency domain analysis of the Gulf Stream data it was shown that the meridional component of velocity at 4000 meters in the 30 day band is associated with westward propagating wave motions. It was pointed out that it is this component which is most coherent with motions at 30 day periods on the Rise. In this section the hypothesis that small amplitude westward propagating meanders of the Gulf Stream can directly excite motions in the far field is explored. This mechanism of a corrugated moving boundary forcing far field motions was first explored by Pedlosky (1977). The condition for radiation of energy away from the boundary was that the phase speed of the boundary must match that of the free waves in the far field. If it can be shown that the westward propagation is associated with the Gulf Stream itself, and not the surrounding eddy field, then this mechanism might be responsible for part of the low frequency energy observed on the Rise.

This possibility that a westward moving wavelike southern boundary is producing the motions observed was first examined by dividing the current record at mooring 780 into down-stream and cross-stream coordinates and using these in a recalculation of the horizontal modes on the Rise. If meanders are responsible for the observed waves, far field motions would be expected to be excited by cross-stream motions and the response would be barotropic provided that the direction of the shear does not change significantly over the depth. As the observed motions are nearly barotropic, and the coherent velocity component is meridional and therefore essentially cross-stream, this hypothesis appears quite plausible.

The down-stream record was constructed by finding the direction of the shear between the 500 and the 1000 meter instruments for each day, and calculating the component of the flow in that direction (Hall and Bryden, 1985). The horizontal modes from the ABCE records were then recalculated after replacing the east and north components of the velocity from mooring 780 by down- and cross-stream coordinates. The 500, 1500 and 4000 meter instruments from all moorings were used, however the upper level records were downweighted in the coherence matrix by 75 percent with the intent of recovering the deep horizontal modes on the Rise. The coordinate systems on the Rise were rotated as in earlier analyses. The results from the 17, 30

and 120 day bands are shown in tables 3.2 through 3.4. The waves on the Rise are essentially the same as those observed in the previous horizontal analysis. The values for amplitude and coherence are the only relevant numbers for the Stream components as phase is difficult to interpret for a component which changes direction daily. The coherence clearly shows that the cross-stream component is more coherent with the modes on the Rise than is the down-stream component, except in the 120 day band.

While it has been demonstrated that the far field waves are coherent with the meridional or cross-stream component of the flow at mooring 780, it has not been shown that meanders and not the background eddy field are responsible for the association. What follows is an attempt to isolate the Stream and the eddy field to examine this problem. In section 3.1 two flow regimes were described. The Stream, at a time when it follows a relatively smooth path to the east, is sampled by the northernmost instruments after December, 1983. These parts of the records will be referred to as the Stream segments. At these same moorings the first parts of the records were dominated by strong meanders and rings. These will be referred to as the ring segments of the records.

Record lengths at mooring 780 were longer than those from the SME array and therefore these series were used to examine the vertical structures of the two segments. The records were split at 285 days and the vertical modes were calculated for each section. The resulting modes are shown in figure 3.10. The amplitudes of the modal velocities at all levels are comparable in the two modes. Also, the vertical phase shifts are negligible in both and the orientations of the ellipses in both are primarily cross-stream. The major dissimilarity is the phase difference between velocity components. In the mode from the Stream segment of the record the motions are more transverse and in the cross-stream plane while those from the ring segment of the record are more rotary. The latter part is more likely to be a single wavelike feature with velocity components nearly in or out of phase. Referring back to the modal ellipses from the horizontal and vertical analyses of sections 2.2.1 and 2.2.2 and comparing to these results shows that while the vertical structure of the whole record (figure 2.7) appears to be a combination of these two structures with possibly more similarity to the mode of the first part, the deep horizontal modal ellipse (figure 2.13) is much more similar in character to the mode constructed from the Stream

inst.	depth	amp u	coh u	ph u	amp v	coh v	ph v
7751	500	1.00	49	0	0.65	21	-109
7752	1500	0.54	44	4	0.57	31	-114
7753	4000	0.66	40	-8	0.31	18	-83
7762	500	4.75	61	-146	1.67	23	53
7764	1500	3.31	77	-141	2.30	59	44
7765	4000	3.09	87	-157	2.84	79	32
7771	4000	3.67	73	-148	5.54	80	70
7781	4000	2.19	70	172	2.86	81	14
7791	4000	3.11	67	164	4.19	87	-36
7802	500	4.89	44	-103	2.37	72	95
7805	1500	5.13	75	-43	2.36	71	107
7806	4000	3.60	75	-60	1.94	70	105

Table 3.2: Horizontal and vertical empirical mode in the 120 day band. Records from mooring 780 are of down- and cross-stream components of velocity, while those from the remaining moorings are of components along and across 64 degrees counterclockwise of east. As in the previous Rise mode in this band, motions at mooring 775 are unrelated to those in the rest of the array. A coherence value of 62 is significant at the 95 percent confidence level.

segment of the record.

To further examine this idea that the Stream segment is related to motions on the Rise, the deep Rise modes were recalculated using each of these two segments of the records. All deep records were divided at 285 days. The 20 and 30 day bands show significant first modes for the Stream segments of the records, while the the modes constructed from the ring segments of the records are no longer significant in these bands since they no longer explain twice as much variance as the second modes (figure 3.11). In addition, coherence values at mooring 780 are very low in the latter analysis. The modal ellipses in the 20 and 30 day bands calculated using the Stream segment of the records are shown in figures 3.12 and 3.13. The modes are similar to those described in section 2.2.2 although in this

inst.	depth	amp u	coh u	ph u	amp v	coh v	ph v
7751	500	0.50	49	0	0.72	70	125
7752	1500	0.75	59	-10	0.65	63	138
7753	4000	2.15	72	-52	1.05	58	132
7762	500	3.21	65	172	1.67	53	-17
7764	1500	1.96	71	153	2.33	70	-28
7765	4000	2.18	76	156	1.97	72	-40
7771	4000	1.32	62	155	1.80	69	2
7781	4000	1.49	80	107	1.72	88	-43
7791	4000	1.05	40	36	1.91	55	-98
7802	500	1.24	23	162	1.44	73	14
7805	1500	0.69	20	142	1.84	73	8
7806	4000	1.21	51	-133	1.51	69	9

Table 3.3: Horizontal and vertical empirical mode in the 30 day band using down- and cross-stream components from mooring 780. The u and v coordinates of the remaining series are along and across 41 degrees counterclockwise of east.

case coherence values are higher and motions are more transverse on the Rise (see tables 3.5 and 3.6). The coherence values at mooring 780 are slightly reduced in the 30 day band which might be explained by the larger bandwidth of these modes. Note the meridional orientation of the ellipses at mooring 780 in both bands.

To further examine the horizontal Stream structure in the two flow regimes it is tempting to divide the records from the SME moorings into two pieces as was done at mooring 780. Unfortunately, the latter parts of the records which sample the eastward flowing Stream is only 5 months in length at most moorings. This was attempted but the results for the 30 day band were not illuminating probably because the bandwidths needed for the desired accuracy were so large. Therefore, instead of examining the frequency domain structure, the records of the meridional components of velocity were examined in the time domain. Figure 3.14 shows the north component of velocity from the 4000 meter instruments at moorings 780, 561,

inst.	depth	amp u	coh u	ph u	amp v	coh v	ph v
7751	500	0.41	44	0	0.10	22	-60
7752	1500	0.43	53	-11	0.18	39	-149
7753	4000	1.28	68	-43	1.00	72	149
7762	500	0.82	40	148	2.66	83	-45
7764	1500	0.37	46	83	1.05	84	-51
7765	4000	0.86	77	85	1.03	92	-60
7771	4000	0.65	58	-68	1.10	59	-61
7781	4000	1.13	79	-14	0.81	61	-105
7791	4000	0.62	50	-76	1.40	84	151
7802	500	0.90	27	92	1.02	60	169
7805	1500	0.36	25	115	0.93	60	175
7806	4000	0.26	14	64	1.09	53	-178

Table 3.4: Horizontal and vertical empirical mode in the 17 day band using down- and cross-stream components from mooring 780. The u and v coordinates of the remaining series are along and across 24 degrees counterclockwise of east.

557, and 559. Westward propagation can be seen between series throughout both time periods described in the text. This is most apparent in the three easternmost moorings of the SME array. It cannot be concluded from examining motions in the time domain that the westward phase propagation is associated with only one of the two flow regimes.

In the last two chapters the general properties of the Gulf Stream in the vicinity of the SME and the ABCE arrays have been described. In the frequency domain particular emphasis was placed on the description of motions in the 30 day band and a possible connection between this mode and waves on the Continental Rise was suggested. The possibility that small amplitude meanders can generate motions in the far field was further explored by examining the two regimes of flow of the Gulf Stream separately. It was found that in the frequency domain the Stream segment of the record is more clearly associated with the motions on the Rise that were described in the chapter 2. In the time domain it was observed that

Inst.	30 days		20 days	
	coh <i>u</i>	coh <i>v</i>	coh <i>u</i>	coh <i>v</i>
7753	81	77	67	74
7765	78	82	85	88
7771	57	70	69	50
7781	79	97	78	92
7791	71	84	42	81
7806	51	59	83	59

Table 3.5: Coherence amplitudes between data series and modal series calculated from the Stream segments of the ABCE records (days 286–507). An amplitude of 67 is significant at the 95 percent confidence level. The coordinate system used is 41 degrees counterclockwise of east.

Inst.	30 days		20 days	
	coh <i>u</i>	coh <i>v</i>	coh <i>u</i>	coh <i>v</i>
7753	66	59	44	31
7765	71	48	82	17
7771	55	36	56	57
7781	89	87	84	85
7791	69	89	88	93
7806	47	36	36	41

Table 3.6: Coherence amplitudes between data series and modal series calculated from the ring segments of the ABCE records (days 1–285). An amplitude of 59 is significant at the 95 percent confidence level. The coordinate system used is 41 degrees counterclockwise of east.

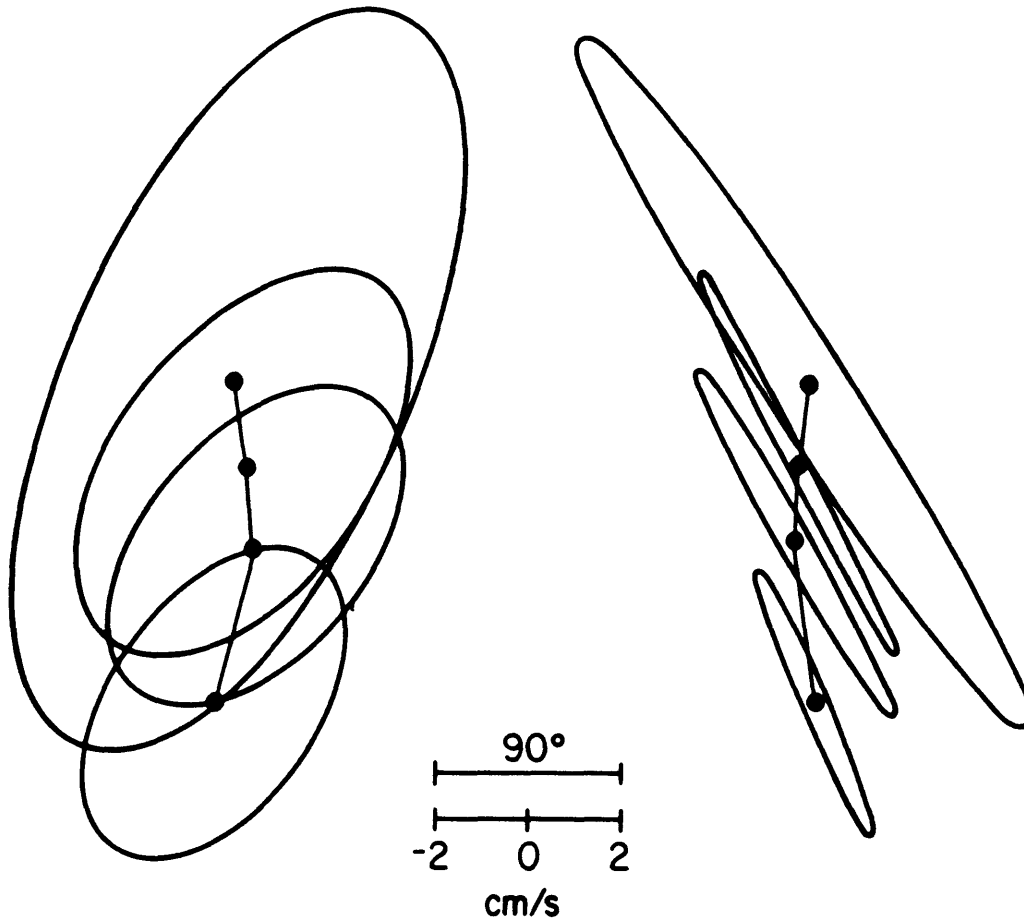


Figure 3.10: Vertical structure at mooring 780 in the 30 day band. a. The mode calculated from the first 285 days of the record when rings and strong meanders dominate the record. b. The mode calculated from the Stream segment of the record when meanders are relatively small in amplitude.

the westward propagation of the meridional component of velocity occurs throughout the record, not just during the Stream segment. These results will be summarized and various problems with this interpretation of the forcing will be addressed in the concluding chapter.

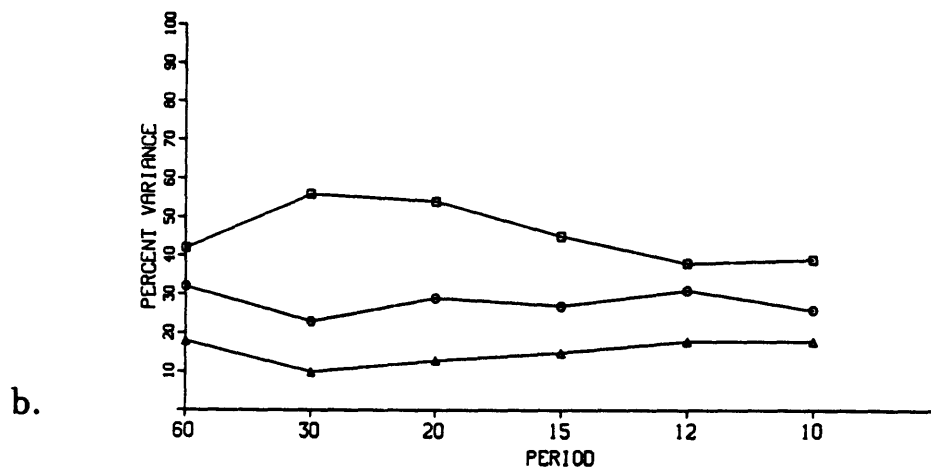
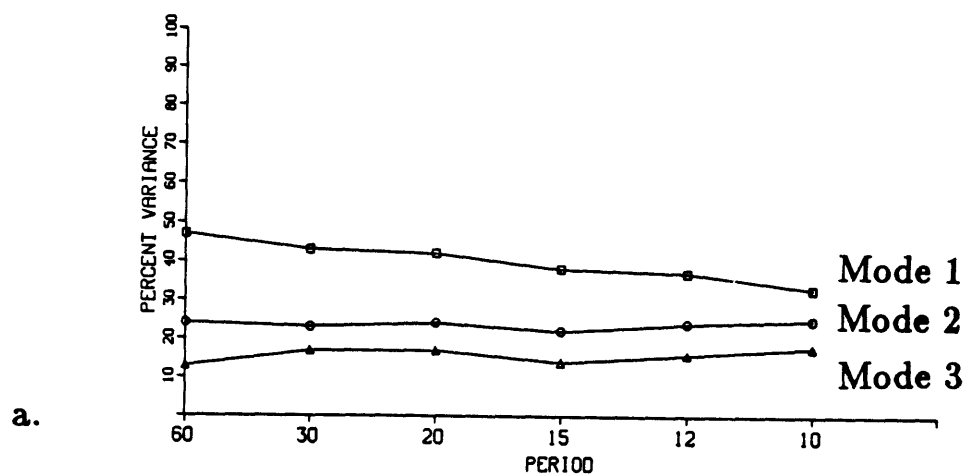


Figure 3.11: Percent variance explained by the first three modes calculated from the split records on the Rise. a. Ring segment. b. Stream segment.

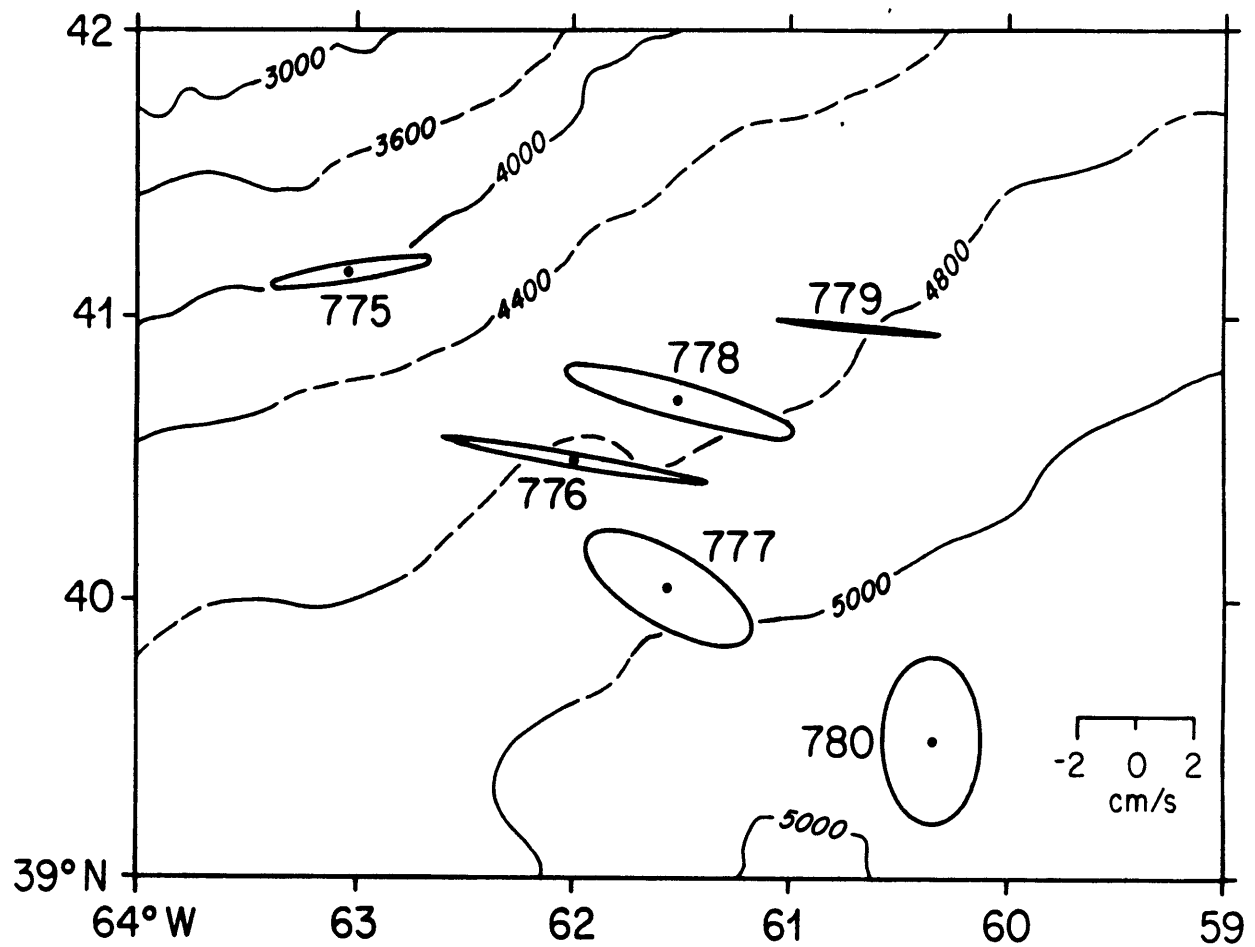


Figure 3.12: Variance ellipse representation of the Stream segment in the 30 day band.

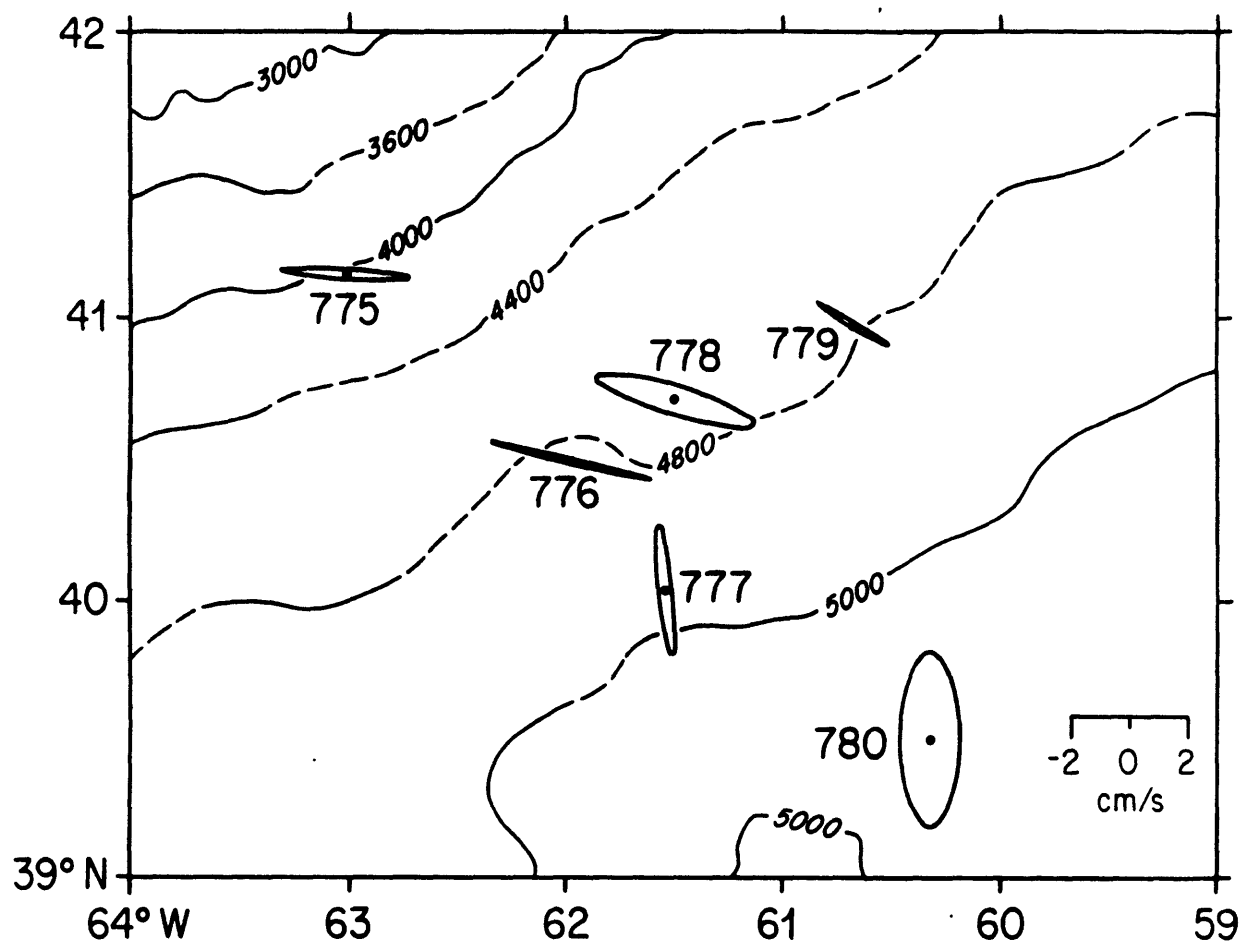


Figure 3.13: Variance ellipse representation of the Stream segment in the 20 day band.

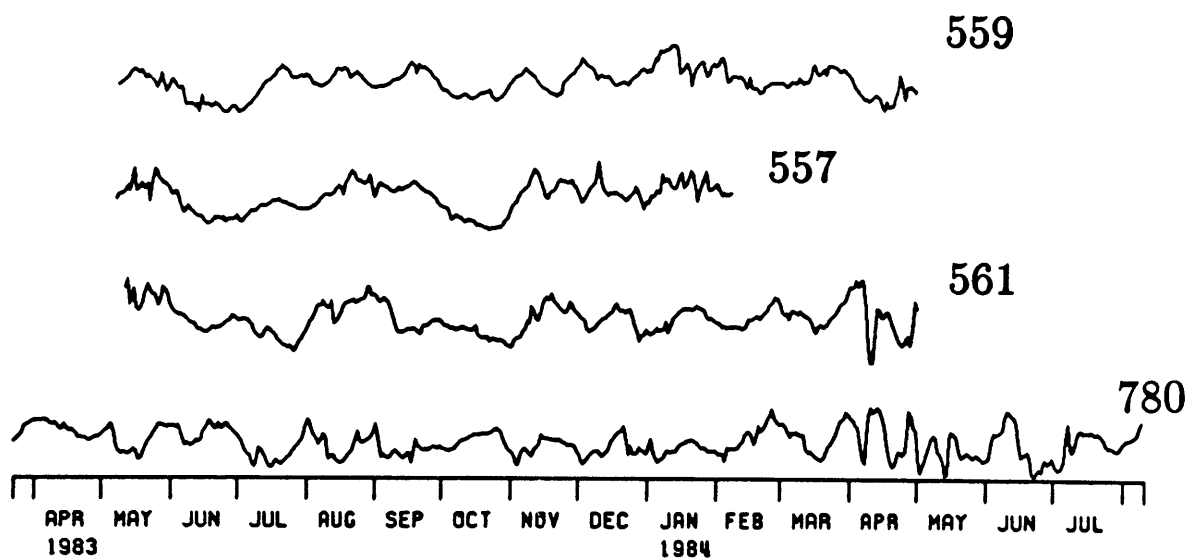


Figure 3.14: Time series of meridional component of velocity at moorings 780, 561, 557, and 559.

Chapter 4

Discussion

Using current meter data collected in the Abyssal Circulation Experiment, deep motions from a region including the Gulf Stream and extending north to the base of the Continental Rise have been described. Gulf Stream variability was examined by supplementing this data set with data collected in the Synoptic Mapping Experiment. The possibility that Rise motions are associated with Stream variability was then explored.

A visual examination of current time series (figure 2.3) revealed the character of motions in three locations—in the Gulf Stream (mooring 780), on the base of the Continental Rise where the bottom slope is relatively large (mooring 775), and at an intermediate position between these two locations (mooring 776). Bottom motions at mooring 780 are to the east and are most often the deep manifestations of a vertically coherent Gulf Stream feature. Motions at mooring 775 are wavelike and bottom intensified with fluctuations sometimes reversing the direction of the westward mean flow at the deepest instrument level. Motions at mooring 776 are of two types. The first is clearly related to the passage of a Gulf Stream feature over the mooring site. Such events are surface intensified and often reverse the direction of the bottom flows. The second type is a nearly barotropic disturbance that does not coincide with the presence of a Gulf Stream feature at the mooring site.

In the frequency domain analysis of the vertical structure at the three moorings 775, 776 and 780 (figures 2.8, 2.7, and 2.6), motions in three bands centered at 17, 30 and 120 day periods were described in detail. At all locations high coherence amplitudes were observed throughout the water column. In the 17 and 30 day modes calculated from current records

from mooring 780 and mooring 776, the variance ellipses show motions of nearly constant amplitude below 500 meters. In the 120 day band there is slightly more decay with depth at mooring 780 but coherence amplitudes are relatively constant throughout the water column. In all bands there is significant amplification of current amplitude at the 500 meter level at the two moorings. At mooring 776 the modes were recalculated after removing Gulf Stream related variability from the 500 meter record and the resulting mode was nearly constant in amplitude at all instrument levels (figure 2.10). It was concluded that the original mode at that instrument is composed of both types of disturbances observed in the time domain and described above. At mooring 775 motions are much more confined to the deepest instrument level. Motions at the upper instrument levels are usually coherent with deep motions but the magnitudes of these currents are much reduced.

In an analysis of the deep horizontal structure over the region sampled by the ABCE instruments, motions at 4000 meters were found to be coherent over the entire array including the Gulf Stream region in a number of frequency bands. Again, the three bands identified above were examined in detail (figures 2.12– 2.14). A comparison to topographic wave theory using realistic parameters for three mooring sites and using buoyancy frequency profiles calculated from CTD data collected near each site revealed that the observed waves exhibit properties of nearly barotropic topographic Rossby waves. The direction of phase propagation is to the southwest in all bands indicating that energy propagation is directed shoreward. This is suggestive of forcing in the vicinity of the Gulf Stream and this possibility was explored.

It has already been stated that a portion of the deep variability at mooring 776 can be attributed to the presence of a Gulf Stream feature over the mooring site. On the other hand, much of the variability is coherent over large horizontal scales and in particular with wave motions at moorings where there is no direct Stream influence, for example mooring 775. It was therefore concluded that the Stream process which is responsible for the majority of the motions on Continental Rise is a more remote process.

It was also concluded that radiating instabilities from the Stream as described in the linear model formulated by Talley (1982) do not play a major role in far field wave generation. Currents in the Stream are to the

east at all depths and the zonal phase speeds of waves generated by this process are therefore to the east. The zonal phase speeds of the observed waves are to the west as they should be in a westward current.

When empirical modes were calculated from 4000 meter records from the Gulf Stream it was found that a significant mode existed only in the band centered at 30 days. A mechanism of Gulf Stream wave generation was suggested which was consistent with the structure of the empirical mode in this band. Specifically, the hypothesis that small amplitude westward propagating meanders of the Stream could directly excite free waves in the far field was explored. Several pieces of evidence in the data support this hypothesis. Westward propagation is observed in the meridional component of the velocity at the 4000 meter instruments in the Gulf Stream. The zonal wavenumber calculated from the phase propagation of this component matches that calculated for the far field waves. In addition, it is the meridional component of the velocity at the Gulf Stream mooring from the ABCE array which was coherent with motions on the Rise in the 30 day band. Finally, when the records from the ABCE data set were divided into two segments, the ring segment and the Stream segment, it was found that records from the Stream mooring, 780 and the mooring furthest up the Rise, 775, are coherent only with the mode calculated from the Stream segment of the records. This is a record of the Gulf Stream during a period when meanders are small in amplitude. The ring segment is a record of strong meanders and rings.

There are questions which remain concerning this interpretation of the forcing. One problem concerns the likelihood of the existence of westward propagating meanders. If the instability process is instrumental in the formation of these disturbances of the jet then the expected direction of phase propagation is to the east. The mechanism proposed by Csanady and outlined in chapter 1 could generate fluctuations with the observed phase properties. If rings are pinched off near mooring 780 then westward propagating Rossby wave-like disturbances in the jet could result. Additionally, the work of Malanotte-Rizzoli, Haidvogel, and Young (1987) showed that eastward or stationary time dependent meanders can effectively excite westward propagating transient responses in both the near and the far field.

Virtually all meanders observed in the satellite data, however, propagate to the east, including those with small amplitudes (Fofonoff, personal

inst.	depth	amp u	coh u	ph u	amp v	coh v	ph v
5611	500	11.12	88	0	2.95	24	268
5612	900	5.03	92	6	2.61	50	255
5614	4000	3.08	85	-9	2.50	65	257
5571	445	7.49	65	24	3.89	36	219
5572	850	4.37	87	19	1.67	37	213
5573	1350	4.14	90	21	1.59	48	202
5574	4000	3.11	86	17	1.49	61	170
5592	900	3.02	70	32	3.20	60	126
5593	1400	3.04	84	35	2.53	56	116
5594	4000	2.50	84	25	2.30	62	115

Table 4.1: Amplitudes, coherence values, and phases of velocity components associated with the first Gulf Stream 30 day mode constructed from all records from moorings 561, 557 and 559. A coherence amplitude of 53 is significant at the 95% confidence level. The mode explains 48% of the variance.

communication). Westward propagation of the front is observed at the surface only preceding the formation of a ring. To examine the vertical structure of the westward propagating disturbances, all records from three Gulf Stream moorings, 561, 557, and 559 were used to construct empirical modes. This analysis showed that the meridional component of velocity over the entire water column in the Stream is actually divided between two modes in the 30 day band (see tables 4.1 and 4.2). The first mode shows the westward propagation at 4000 meters described in the previous chapter. Meridional components of velocity at 500 meters are not significantly coherent with this mode. It is interesting that the amplitude explained by the mode at the upper level instruments is reduced to that at the deeper instruments because of low coherence amplitudes. If phase values could be believed westward propagation of a nearly barotropic disturbance would be observed in the data. However, most of the variance in the meridional component of the velocity at the upper instrument level is explained by the second empirical mode. This mode is characterized by strong surface intensification and *eastward* phase propagation. The westward propagation

inst.	depth	amp u	coh u	ph u	amp v	coh v	ph v
5611	500	3.02	24	0	9.71	80	97
5612	900	0.86	16	61	4.03	78	94
5614	4000	0.78	22	115	2.38	62	87
5571	445	3.40	29	66	7.81	71	142
5572	850	1.20	24	47	3.34	74	130
5573	1350	0.16	3	12	2.05	62	138
5574	4000	0.28	8	140	0.64	26	138
5592	900	1.86	43	49	2.21	41	243
5593	1400	0.43	12	21	1.64	37	249
5594	4000	0.13	4	-21	0.90	24	225

Table 4.2: Amplitudes, coherence values, and phases of velocity components associated with the second Gulf Stream 30 day mode constructed from all records from moorings 561, 557 and 559. A coherence amplitude of 53 is significant at the 95% confidence level. The mode explains 20% of the variance.

observed at 4000 meters could therefore be the bottom manifestation of a Gulf Stream meander which is obscured in the upper water column by surface trapped eastward propagating features. On the other hand, it could be westward propagating eddies beneath the Stream. This question remains unanswered.

An additional problem is the limited amount of evidence that was cited to support the interpretation of the forcing outlined above. Westward propagation under the Stream was observed in just one frequency band. Large scale coherence in this band was further limited to the Stream segment of the record. One would expect that if this is an important wave generation mechanism, it would also be occurring during the early part of the record when the Stream is simply displaced to the south of mooring 780. Both of these problems may be related to difficulties in interpretation of empirical modes and therefore attributed to the limitations of the method employed in the analysis. Because the significance of the empirical modes is based on the amount of variance explained by one mode relative to the next, wave structures in regions in which multiple processes are occurring are more difficult to interpret. If a first mode is not significant—if the variance is more evenly split between the first few modes—this may only indicate that more than one important process is present in the data. There is no guarantee that each mode will describe one process as they are not necessarily orthogonal, and more likely each mode will be a combination of processes. This is most likely occurring in the Gulf Stream vicinity, especially during periods of strong ring activity. The problem is further complicated by the necessarily broad bandwidths resulting from short record lengths. Therefore, if the meander mechanism outlined above is occurring in conjunction with other generation mechanisms such as dispersal from Gulf Stream rings, then interpretation using this method is more difficult. The method is better suited to periods of relatively low variability such as in the Stream segment of the records.

This investigation has focused on frequency bands which showed a clear association between motions on the Rise and motions in the vicinity of the Gulf Stream mooring, 780. One question which should be addressed is whether the Rise variability that has been linked to Gulf Stream wave generation mechanisms represents a significant amount of the total variability. The problem that the complexity of motions in the Stream vicinity reduces

inst.	depth	amp u	coh u	ph u	amp v	coh v	ph v
7753	4000	2.45	81	0	1.65	89	179
7765	4000	2.46	65	128	1.03	43	-60
7771	4000	1.41	42	-164	0.20	6	163
7781	4000	2.25	90	139	1.48	52	0
7791	4000	3.23	82	120	1.71	85	-55
5584	4000	1.85	90	144	4.02	93	30

Table 4.3: Amplitudes, coherence values, and phases of velocity components associated with the 60 day horizontal mode including records from mooring 558. The coordinate system used is 41 degrees north of east. A coherence amplitude of 62 is significant at the 95 percent level.

the coherence with the Gulf Stream record has already been discussed. In addition, waves may be generated further downstream or upstream of mooring 780 and coherence with mooring 780 records may be low. In some frequency bands not previously described, topographic waves were observed which were coherent over the array with the exception of mooring 780. It might be concluded that these motions are not generated by Stream processes. However, strong coherence between motions at mooring 558 in the SME array and motions at the more eastward ABCE moorings, including mooring 775, is observed in both the 40 and 60 day bands (see tables 4.3 and 4.4). Because of the shorter record length it is not easy to examine this result in the two flow regimes separately and it cannot be concluded that the waves in these bands are associated with one specific Gulf Stream process. However, the connection to the Gulf Stream in these two additional bands allows for the conclusion that a significant fraction of the low frequency variability in the ABCE records has been linked with and was most likely generated by the Gulf Stream.

A second year of data was collected in the SME which was not yet available to include in this study. As many of the problems in interpretation of the source region structure were caused by the shorter records in the SME, it would be interesting to include the second year in the analysis. This would permit an examination of the horizontal structure of the Stream seg-

inst.	depth	amp u	coh u	ph u	amp v	coh v	ph v
7753	4000	2.71	86	0	1.72	88	-174
7765	4000	2.16	68	169	1.54	53	-25
7771	4000	1.70	62	-161	0.56	21	39
7781	4000	2.55	93	173	2.56	83	9
7791	4000	3.31	73	131	1.59	80	-36
5584	4000	1.79	76	142	3.32	91	31

Table 4.4: As in table 4.3 in the 40 day band.

ment of the records in the frequency domain. The reduction of bandwidths would allow for a more careful comparison to Rise modes calculated from ABCE data. In addition, this reduction in bandwidth might reduce the complexity of the motions in each frequency band and an interpretation of the source region structure might be possible in more than one band.

In conclusion, there is a significant amount of low frequency variability on the Continental Rise in the western North Atlantic in the form of topographic Rossby waves. It is apparent from this investigation that a large fraction of this variability is generated by Gulf Stream forcing mechanisms. Although it is likely that a number of processes in the Gulf Stream can excite these motions, the results of this study pointed to one possibility, namely, that westward propagating meanders can directly excite far field waves.

References

- Csanady, G.T., 1985. Radiation of topographic waves from Gulf Stream meanders. Accepted for publication in *Continental Shelf Research*.
- Dickinson, R.E., and F.L. Clare, 1973. Number of unstable modes of a hyperbolic-tangent barotropic shear flow. *J. Atmos. Sci.*, **30**, 1035–1049.
- Flierl, G.R., 1977. The application of linear quasigeostrophic dynamics to Gulf Stream rings. *J. Phys. Oceanogr.*, **7**, 365–379.
- Hall, M.M., and H.L. Bryden, 1985. Profiling the Gulf Stream with a current meter mooring. *Geophys. Res. Letters*, **12**, 203–206.
- Hogg, N.G., 1981. Topographic waves along 70°W on the Continental Rise. *J. Mar. Res.*, **39**, 627–649.
- , 1983. A note on the deep circulation of the western North Atlantic: its nature and causes. *Deep Sea Res.*, **30**, 945–961.
- , R.S. Pickart, R.M. Hendry, W. Smethie, Jr., 1986. The Northern Recirculation Gyre of the Gulf Stream. *Deep Sea Res.*, **33**, 1139–1165.
- , and H. Stommel, 1985. On the relation between the deep circulation and the Gulf Stream. *Deep Sea Res.*, **32**, 1181–1193.
- Johns, W.E., and D.R. Watts, 1986. Time scales and structures of topographic Rossby waves and meanders in the deep Gulf Stream. *J. Mar. Res.*, **44**, 267–290.
- Kelley, E.A., and G.L. Weatherly, 1985. Abyssal eddies near the Gulf Stream. *J. Geophys. Res.*, **90**, 3151–3159.
- Kroll, J., 1979. The kinetic energy on a continental shelf from topographic Rossby waves generated off the shelf. *J. Phys. Oceanogr.*, **9**, 712–722.
- Louis, J.P., B.D. Petrie, and P.L. Smith, 1982. Observations of topographic Rossby waves on the continental margin off Nova Scotia. *J. Phys. Oceanogr.*, **12**, 47–55.
- Louis, J.P., and P.C. Smith, 1982. The development of the barotropic radiation field of an eddy over a slope. *J. Phys. Oceanogr.*, **12**, 56–73.
- Malanotte-Rizzoli, P., 1984. Boundary-forced nonlinear planetary radiation. *J. Phys. Oceanogr.*, **14**, 1032–1046.
- Malanotte-Rizzoli, P., D.B. Haidvogel, and R.E. Young, 1987. Numerical simulation of transient boundary forced radiation. Part I: The linear regime. In press in *J. Phys. Oceanogr.*.

- Malanotte-Rizzoli, P., R.E. Young, and D.B. Haidvogel, 1987. Numerical simulation of transient boundary forced radiation. Part II: The modon regime. In press in *J. Phys. Oceanogr.*.
- Pedlosky, J., 1977. On the radiation of mesoscale energy in the mid- ocean. *J. Mar. Res.*, **24**, 591-600.
- , 1980. The destabilization of shear flow by topography. *J. Phys. Oceanogr.*, **10**, 1877-1880.
- Rhines, P.B., 1970. Edge-, bottom-, and Rossby waves in a rotating stratified fluid. *Geophys. Fluid Dyn.*, **1**, 273-302.
- , 1971. A note on the long-period motions at Site D. *Deep Sea Res.*, **18**, 21-26.
- Talley, L.D., 1982. Instabilities and radiation of thin baroclinic jets. *PhD thesis, Joint Program in Oceanography and Ocean Engineering, Woods Hole Oceanographic Institution*. 233 pp.
- , 1983a. Radiating barotropic instability. *J. Phys. Oceanogr.*, **13**, 972-987.
- , 1983b. Radiating instabilities of thin baroclinic jets. *J. Phys. Oceanogr.*, **13**, 2161-2181.
- Thompson, R.O.R.Y., 1977. Observations of Rossby waves near site D. *Progress in Oceanography*, **7**, 135-162.
- Tucholke, B.E., C.D. Hollister, P.E. Biscaye, and W.D. Gardner, 1985. Abyssal current character determined from sediment bedforms on the Nova Scotian Continental Rise. *Marine Geology*, **66**, 43-57.
- Wallace, J.M., and R.F. Dickinson, 1972. Empirical orthogonal representation of time series in the frequency domain. Part I: theoretical considerations. *J. Appl. Meteor.*, **11**, 887-892.
- Weatherly, G.L., and E.A. Kelley, 1985. Storms and flow reversals at the Hebble site. *Marine Geology*, **66**, 205-218.